

# Endothelial Insulin Resistance of Freshly Isolated Arterial Endothelial Cells From Radial Sheaths in Patients With Suspected Coronary Artery Disease

Nobuyuki Masaki, MD; Yasuo Ido, MD; Toshiyuki Yamada, MD; Youhei Yamashita, MD; Takumi Toya, MD; Bonpei Takase, MD; Naomi M. Hamburg, MD; Takeshi Adachi, MD

**Background**—Endothelial insulin resistance is insulin-insensitivity in the vascular endothelium and can be observed in experimental models. This study aimed to investigate endothelial insulin resistance in patients with suspected coronary artery disease. To this end, a novel method of obtaining freshly isolated arterial endothelial cells from a radial catheter sheath was developed.

**Methods and Results**—Freshly isolated arterial endothelial cells were retrieved from catheter sheaths placed in radial arteries for coronary angiography (n=69, patient age  $64\pm 12$  years). The endothelial cells were divided into groups for incubation with or without insulin, vascular endothelial growth factor, or acetylcholine. The intensity of phosphorylated endothelial nitric oxide synthase at Ser1177 (p-eNOS) was quantified by immunofluorescence microscopy. The percentage increase of insulin-induced phosphorylated endothelial nitric oxide synthase correlated negatively with derivatives of reactive oxygen metabolites, an oxidative stress test ( $r=-0.348$ , n=53,  $P=0.011$ ), E/E', an index of left ventricular diastolic dysfunction in Doppler echocardiography ( $\rho=-0.374$ , n=49,  $P=0.008$ ), and log-transformed brain natriuretic peptide ( $r=-0.266$ , n=62,  $P=0.037$ ). Furthermore, percentage increase of insulin-induced p-eNOS was an independent factor for the cardio-ankle vascular index (standardized coefficient  $\beta=-0.293$ , n=42,  $P=0.021$ ) in the multivariate regression analysis of adaptive least absolute shrinkage and selection operator.

**Conclusions**—Our results suggested that endothelial insulin resistance is associated with oxidative stress, left ventricular diastolic dysfunction, heart failure, and arterial stiffness. (*J Am Heart Assoc.* 2019;8:e010816. DOI: 10.1161/JAHA.118.010816.)

**Key Words:** arterial stiffness • endothelial nitric oxide synthase • insulin resistance

Insulin resistance (IR) is classically defined as the impaired action of insulin in organs responsible for glucose metabolism, including adipose tissue, skeletal muscle, and the liver.<sup>1</sup> In IR, insulin-mediated glucose uptake is reduced in muscles and adipocytes. Moreover, hepatic gluconeogenesis

and lipogenesis are increased, whereas lipolysis occurs in adipose tissue. However, a more comprehensive concept includes insulin-insensitivity in other organs that are regulated by insulin but not directly involved in the control of blood glucose levels.<sup>2</sup>

Endothelial IR is insulin-insensitivity in the vascular endothelium and is considered peripheral IR.<sup>3</sup> Insulin directly stimulates the release of nitric oxide (NO) from the endothelium by activating insulin receptor substrate (IRS)-1, which leads to phosphatidylinositol 3-kinase (PI3K)-protein kinase B (Akt)-mediated phosphorylation of endothelial NO synthase (eNOS).<sup>4–7</sup> NO promotes vasodilatation and prevents leukocyte adhesion,<sup>8</sup> thrombocyte aggregation,<sup>9</sup> and smooth muscle cell proliferation.<sup>10</sup> Therefore, when the action of insulin is reduced in the endothelium, it is thought to be associated with endothelial dysfunction and other vascular diseases.

At present, the definition of endothelial IR is almost equal to deterioration of IRS-1/PI3K/Akt/eNOS signaling, which can be observed only in experimental models using

From the Departments of Intensive Care Medicine (N.M., B.T.) and Cardiology (Y.I., Y.Y., T.T., T.A.), National Defense Medical College, Tokorozawa, Japan; Department of Cardiovascular Surgery, Keio University Graduate School of Medicine, Tokyo, Japan (T.Y.); The Whitaker Cardiovascular Institute, Department of Medicine, Boston University School of Medicine, Boston, MA (N.M.H.). Accompanying Data S1 and Figures S1 through S7 are available at <https://www.ahajournals.org/doi/suppl/10.1161/JAHA.118.010816>

**Correspondence to:** Nobuyuki Masaki, MD, Department of Intensive Care Medicine, National Defense Medical College, 3-2 Namiki, Tokorozawa-shi, Saitama 352-8165, Japan. E-mail: [masakinobuyuki@hotmail.com](mailto:masakinobuyuki@hotmail.com)

Received September 4, 2018; accepted February 12, 2019.

© 2019 The Authors. Published on behalf of the American Heart Association, Inc., by Wiley. This is an open access article under the terms of the Creative Commons Attribution License, which permits use, distribution and reproduction in any medium, provided the original work is properly cited.

## Clinical Perceptive

### What Is New?

- We developed a new non-invasive method to collect human freshly isolated arterial endothelial cells from radial catheter sheaths, which are disposable devices for coronary angiography.
- Using the freshly isolated arterial endothelial cells, endothelial insulin resistance, defined as reduced insulin-induced endothelial nitric oxide synthase activation via insulin receptor substrate-1/phosphatidylinositol 3-kinase/protein kinase B/endothelial nitric oxide synthase signaling, was assessed by immunofluorescent microscopy.

### What Are the Clinical Implications?

- Endothelial insulin resistance was associated with non-diabetic factors including oxidative stress, heart failure, and arterial stiffness assessed by cardio-ankle vascular index.

endothelial cells or animals.<sup>2</sup> The concept of endothelial IR has not been clinically established because only a small number of studies have shown the actual response to insulin in endothelial cells of patients with metabolic disorders to date.<sup>11,12</sup> Many clinical studies have reported that IR decreases NO synthesis in the endothelium. However, the assessments in these studies were based on metabolic IR, for example the homeostatic model assessment of insulin resistance.<sup>13</sup> Thus, if possible, it is preferable to evaluate endothelial IR for this purpose. Therefore, we have developed a novel method of obtaining endothelial cells from patients. We collected arterial endothelial cells from radial catheter sheaths, which are disposable devices for coronary angiography. This does not require any additional invasive procedures and can be used in many patients.

The aim of this study was to explore the influential factors of endothelial IR using our novel method because IRS-1/PI3K/Akt/eNOS pathway can be deteriorated by various factors. Our hypothesis is that endothelial IR may occur in patients with not only diabetes mellitus but also cardiovascular disease which can cause endothelial dysfunction such as heart failure and atherosclerosis. We considered eNOS responses to insulin as an index of endothelial IR,<sup>11,12</sup> and compared them with laboratory examination, echocardiographic parameters, and the cardio-ankle vascular index (CAVI). Lower amplification of insulin-induced phosphorylated endothelial NO synthase at Ser1177 (p-eNOS) has been shown to be an indicator of insufficient NO production.<sup>12</sup> CAVI is an indicator of arterial stiffness that excludes the effect of blood pressure at the time of the measurement.<sup>14</sup> In addition, we assessed eNOS responses to vascular endothelial growth factor (VEGF) and acetylcholine.

## Materials and Methods

The authors declare that all supporting data are available within the article and its online supplementary files. Additional methods and results can be found in Data S1.

### Subjects

Patients who underwent elective cardiac catheterization from January 2017 to December 2017 at the National Defense Medical College Tokorozawa, Japan were enrolled in the study. Exclusion criteria included ongoing treatment for malignant tumor and hemodialysis. The study protocol was approved by the National Defense Medical College Review Board, and all participants provided written informed consent.

Hypertension was identified as blood pressure above 140/90 mm Hg or as receiving medication for the condition. Diabetes mellitus (DM) was diagnosed as fasting blood glucose >126 mg/dL or the use of insulin or oral hypoglycemic agents. Hyperlipidemia was defined as total cholesterol >220 mg/dL, low-density lipoprotein cholesterol >140 mg/dL, or receiving anti-hyperlipidemic medication. Estimated glomerular filtration rate (eGFR) was calculated using the Modification of Diet in Renal Disease equation modified for a Japanese population.<sup>15</sup>

### Laboratory Examination

Blood samples were drawn through a guiding sheath during coronary angiography without the administration of heparin or nitroglycerin, collected into plain tubes, and refrigerated immediately. Serum was obtained by centrifugation at 1610g for 10 minutes at 4°C. Derivatives of reactive oxygen metabolites (d-ROMs) were measured in serum using the reactive oxygen metabolites free radical test (Dacron International, Grosseto, Italy). The d-ROMs test was used to quantify total hydroperoxide levels by measuring the ability of transition metals to catalyze the formation of free radicals. Oxidized N,N-diethyl-para-phenylenediamine was detected spectrophotometrically at 505 nm.<sup>16,17</sup> One unit of d-ROMs (U-CARR) corresponds to the amount of hydroperoxide that can be converted by superoxide dismutase to approximately 0.08 mg/dL H<sub>2</sub>O<sub>2</sub>. Homeostatic model assessment of insulin resistance was calculated from fasting insulin levels, as previously described.<sup>18</sup>

### Coronary Angiography

Coronary angiography was performed with a 4 Fr catheter system. Angiograms were taken from at least 4 standard projections for each right and left coronary artery. Coronary artery disease (CAD) was defined as the presence of coronary stenosis of >75% in at least 1 coronary vessel in the angiogram, or a past history of myocardial infarction,

percutaneous coronary intervention, or coronary artery bypass grafting surgery.

## Physiological Tests

Cardio-ankle vascular index (CAVI) was obtained using a VaSera CAVI instrument (Fukuda Denshi Co, Ltd, Tokyo), equipped with electrocardiography, phonocardiography, and mechanocardiography functions. CAVI was recorded in patients after 5 minutes of rest in the supine position. The calculation of CAVI is based on blood pressure and heart-ankle pulse wave velocity, monitoring of heart sounds, and electrocardiography. Heart-ankle pulse wave velocity was calculated by dividing the distance from the aortic valve to the ankle artery by the sum of the time intervals between aortic valve closure sound (first part of the second heart sound) and the notch of the brachial pulse wave, and between the rise of the brachial pulse wave and the ankle pulse wave. CAVI was determined using the following formula,

$$\text{CAVI} = a [2\rho / (\text{Ps} - \text{Pd}) \times \ln(\text{Ps}/\text{Pd}) \times \text{ha PWV}^2] + b$$

where Ps and Pd are systolic and diastolic blood pressure, respectively;  $\rho$  is blood density; and a and b are constants. CAVI was taken as the average of the right and left CAVI values.

A CAVI score of <8.0 is supposed to be normal, whereas a value <9.0 but  $\geq 8.0$  is considered “borderline”. A CAVI  $\geq 9.0$  leads to a diagnosis of suspected arteriosclerosis.<sup>14,19</sup> For the CAVI evaluation, we excluded patients with severe aortic insufficiency, bilateral ankle-brachial index <0.9, or persistent atrial fibrillation (Figure 1) because it is difficult to obtain accurate measurements in such patients.<sup>20</sup>

## Echocardiography

Transthoracic echocardiography was performed by trained sonographers. Peak early diastolic transmitral flow velocity (E) and peak late diastolic transmitral flow velocity (A) phases of mitral inflow were recorded at the mitral valve leaflet tips from an apical 4-chamber view using pulsed Doppler echocardiography. Deceleration time was derived from the early filling wave and left ventricular (LV) myocardial velocity was evaluated at the septal mitral valve annulus. The peak early diastolic annular velocity (E') was measured using tissue-Doppler imaging. The ratio of early mitral filling velocity (E) to E' (E/E') was calculated as an index of LV diastolic dysfunction. The ejection fraction was measured using echocardiography with the Teichholz method or biplane modified Simpson method if appropriate.

## Peripheral Endothelial Cell Collection

An inner dilator of a radial catheter sheath used for coronary angiography was extracted under a sterile technique (Medikit

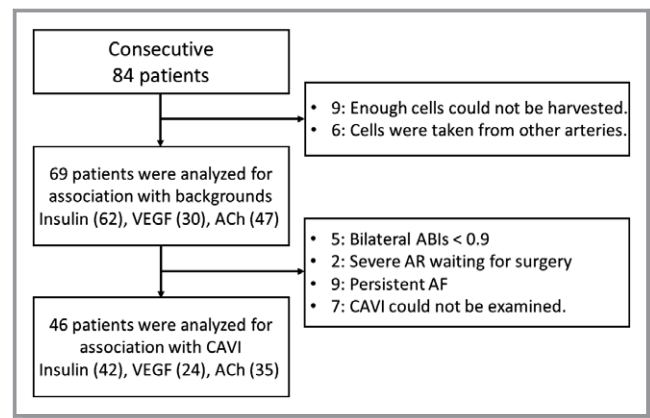


**Figure 1.** Enrollment of the patients. Exclusion criteria are described. Of 84 consecutive patients undergoing coronary angiography, data from 69 patients were analyzed for comparison between the cell study and traditional cardiovascular risk factors. The numbers in parentheses represent patients whose endothelial cells could be examined under biochemical stimulation. Among them, 46 patients met the inclusion criteria for CAVI. ABI indicates ankle brachial index; AF, atrial fibrillation; AR, aortic valve regurgitation; CAVI, cardio-ankle vascular index; VEGF, vascular endothelial growth factor.

Co, Ltd, Japan) as follows. A right wrist was sterilized. A radial artery was punctured by a thin needle with inner lumen. Then, a guidewire was placed into the artery through the needle. A 4 Fr radial catheter sheath was inserted into radial artery along with the guidewire. The inner dilator of the sheath was extracted together with the guidewire from the radial artery. In the laboratory, endothelial cells adherent to the disposable device were removed by washing with an erythrocyte lysing kit (R&D Systems) and the pellet was obtained by centrifugation. The pellet was washed again with endothelial basal medium (EBM-2; Lonza, Basel, Switzerland) and plated on poly-L-lysine-coated microscope slides (Sigma, St. Louis, MO). After the incubation in 5% CO<sub>2</sub> 37° for 30 minutes, the endothelial cells were treated with or without insulin (WAKO: 100 nmol/L, 30 minutes), recombinant human vascular endothelial growth factor (WAKO: 20 ng/mL, 30 minutes), or acetylcholine (Sigma: 1  $\mu$ mol/L, 15 minutes). Next, the cells were fixed immediately in 4% paraformaldehyde and the slides were washed in PBS, dried and stored at  $-80^{\circ}\text{C}$  until further processing. The process from harvesting cells to fixation takes 90 minutes.

## Assessment of Protein Expression by Quantitative Immunofluorescence

Fixed sample slides were thawed and rehydrated with PBS containing 50 mmol/L glycine (Sigma) for 10 minutes. The cells on the slides were permeabilized with 0.1% Triton X-100, and non-specific binding sites were blocked with 0.5% BSA. The slides were incubated overnight at 4°C with primary antibodies against the following targets: phosphorylated eNOS at ser1177

(p-eNOS) (1:200 dilution; GeneTex, Inc, Irvine, CA), total eNOS (1:100 dilution; Millipore, MA), vascular cell adhesion molecule-1 (1:200 dilution; Abcam, Cambridge, MA), vascular endothelial cadherin (1:50; Santa-Cruz, Dallas, TX). All slides were double-stained with anti-von Willebrand Factor (vWF) antibody (1:300 dilution; Thermo Fisher Scientific) for identification of endothelial cells. After incubation, the slides were washed and incubated for 3 hours at 37°C with corresponding Alexa Fluor-488 and Alexa Fluor-594 antibodies (1:200 dilution; Invitrogen, Carlsbad, CA). The slides were washed 3 times and mounted under glass coverslips with Vectashield Antifade Mounting Medium containing DAPI for nuclear identification (Vector Laboratories, Burlingame, CA). For each batch of patient-derived cells, we stained a control slide of human aortic endothelial cells at each staining.

The immunofluorescence intensity was quantified by modifying methods reported previously.<sup>11,12</sup> Slide images were obtained with a fluorescence microscope (BZ-X700, KEYENCE, Japan) at  $\times 40$  magnification. The exposure time was constant at 200 ms for p-eNOS. Fluorescence intensity was quantified by a software program (KEYENCE Corp., Osaka, Japan). Image intensity was corrected for background fluorescence by subtraction. For each protein of interest, fluorescence intensity was quantified in 20 cells from each patient and the means were obtained. Intensity is expressed in arbitrary units (au), which is the percentage of the average fluorescence intensity from the patient sample to the average fluorescence intensity of the human aortic endothelial cells slide stained at the same time. This formula is used to adjust deviations under staining conditions. Quantification was performed with blinding to the identity of the subject.

The percentage change of p-eNOS by each stimulus (insulin, VEGF, acetylcholine) was calculated as follows:

$$\text{Percent change of p-eNOS (\%)} = 100 \times (\text{stimulated p-eNOS} - \text{basal p-eNOS}) / \text{basal p-eNOS}$$

where basal p-eNOS is the intensity of p-eNOS without stimulation.

## Statistical Analyses

The distribution of continuous clinical characteristics and measurements were evaluated by examining a histogram and applying the Shapiro–Wilk test. The 2-group comparisons were performed with *t* test or Mann–Whitney *U* test as appropriate. Categorical clinical characteristics were compared using  $\chi^2$  testing or Fisher exact test if appropriate. The correlation coefficient of 2 variables of normal distribution was obtained with Pearson method. Spearman method was used if at least 1 variable of non-normal distribution was included. The paired *t* test was used for paired samples for immunofluorescent intensities before and after serum stimulation.

Univariate and multivariate regression analyses were performed to identify independent variables associated with CAVI scores from clinical features and the results of cell experiments. In the multivariate analysis, traditional cardiovascular risk factors and the independent factors correlating with CAVI ( $<0.1$ ) in the univariate analysis were included in a crude model (model 1). Next, backward stepwise method was used to select effective explanatory variables from the variables used in model 1 (model 2). In addition, we performed the adaptive least absolute shrinkage and selection operator (Lasso) regression analysis, which is currently considered to obtain a better-fitting model for small size samples (model 3).<sup>21</sup> d-ROMs were not included in the regression models because there was an insufficient number of patients. Statistical analyses were performed using SPSS version 22.0 (SPSS Japan, Tokyo), and JMP pro. version 13.1.0 (SAS Institute Japan, Tokyo) for the adaptive Lasso regression analysis.

Summary data are presented as means  $\pm$  SDs for variables of normal distribution or median (1st quartile, 3rd quartile) for those of non-normal distribution. In all analyses,  $P < 0.05$  was considered statistically significant.

## Results

### Subjects

A total of 84 consecutive patients undergoing coronary angiography were enrolled in this study (Figure 1). Among them, the data of 69 patients were available for the analysis (Table 1). The study population included 39 patients (57%) with coronary artery disease (CAD). Revascularization had been performed in 25 patients. One patient had previously undergone both coronary artery bypass grafting (CABG) and percutaneous coronary intervention (PCI). In addition, CAVI scores were recorded in 46 patients. The average CAVI score was  $8.78 \pm 1.71$  (Table 2).

### Identification of Endothelial Cells

The arterial endothelial cells were identified by microscope by weibel-palade bodies of vWF staining. The vWF positive cell was also probed by antibodies of total eNOS, and p-eNOS Ser1177 (Figure 2A and 2B). We found some cells to be positive for anti-vascular cell adhesion molecule-1 antibody (Figure 2C). The image of vascular endothelial-cadherin was also shown in Figure 2D.

### Quantification of the Immunofluorescent Intensity

The validation of the immunofluorescent quantification was performed using commercialized human umbilical vein



**Table 1.** Clinical Characteristics

|   | Patients (n=69) |
|---|-----------------|
| Age, y                                      | 64±12           |
| Sex (women/men), n (%)                      | 19/50 (28/72)   |
| BMI, kg/m <sup>2</sup>                      | 23±3            |
| Hypertension, n (%)                         | 47 (68)         |
| Hyperlipidemia, n (%)                       | 43 (62)         |
| Diabetes mellitus, n (%)                    | 22 (32)         |
| Current smoking, n (%)                      | 25 (36)         |
| Previous conditions                         |                 |
| CAD, n (%)                                  | 39 (57)         |
| OMI, n (%)                                  | 13 (19)         |
| CABG, n (%)                                 | 5 (7)           |
| PCI, n (%)                                  | 21 (30)         |
| Persistent AF, n (%)                        | 9 (13)          |
| DCM, n (%)                                  | 8 (12)          |
| HCM, n (%)                                  | 2 (3)           |
| Aortic aneurysm, n (%)                      | 5 (7)           |
| Valvular heart disease, n (%)               | 9 (13)          |
| Hospital admission for heart failure, n (%) | 17 (25)         |
| Medications                                 |                 |
| Beta-blocker, n (%)                         | 36 (52)         |
| ACE inhibitor, n (%)                        | 12 (17)         |
| ARB, n (%)                                  | 27 (39)         |
| Calcium channel blocker, n (%)              | 22 (32)         |
| Furosemide, n (%)                           | 17 (25)         |
| Spironolactone, n (%)                       | 13 (19)         |
| Statins, n (%)                              | 42 (61)         |
| Insulin, n (%)                              | 5 (7)           |
| Warfarin, n (%)                             | 9 (13)          |
| P2Y <sub>12</sub> inhibitor, n (%)          | 24 (35)         |
| Aspirin, n (%)                              | 31 (45)         |

Data are expressed as means or counts (%) as appropriate. ACE indicates angiotensin-converting enzyme; AF, atrial fibrillation; ARB, angiotensin receptor blocker; BMI, body mass index; CABG, coronary artery bypass surgery; CAD, coronary artery disease; DCM, dilated cardiomyopathy; HCM, hypertrophic cardiomyopathy; OMI, old myocardial infarction; PCI, percutaneous coronary intervention.

endothelial cells. The results are shown in Figures S1 through S3. We compared the results of Western blotting and immunofluorescence using this antibody (Figure S4). There was a positive linear correlation between the intensities evaluated by the 2 modalities.

In addition, we preformed serum-stimulation to estimate the maximum intensity of p-eNOS Ser1177. It was previously known that thrombin in serum phosphorylates

**Table 2.** Experimental Results of p-eNOS and Laboratory Data

|                                 | Patients (n=69) |
|---------------------------------|-----------------|
| Endothelial experiments         |                 |
| Basal p-eNOS, au                | 41±22           |
| ΔINS, %*                        | 7±31            |
| ΔVEGF, % <sup>†</sup>           | -0.6±30         |
| ΔACh, % <sup>‡</sup>            | 7±39            |
| Physiological examinations      |                 |
| CAVI <sup>§</sup>               | 8.78±1.71       |
| E/E' <sup>  </sup>              | 11 (9, 16)      |
| DCT, ms <sup>¶</sup>            | 209±78          |
| EF (%) <sup>#</sup>             | 63 (43, 73)     |
| Laboratory data                 |                 |
| WBC, /μL                        | 6091±2041       |
| Hemoglobin, g/dL                | 14 (13, 15)     |
| Hematocrit, %                   | 40±5            |
| Platelets, ×10 <sup>4</sup> /μL | 24±7            |
| AST, IU/L                       | 22 (19, 28)     |
| ALT, IU/L                       | 20 (15, 28)     |
| LDL cholesterol, mg/dL          | 94±31           |
| triglyceride, mg/dL             | 108 (83, 167)   |
| HDL cholesterol, mg/dL          | 52±16           |
| Glucose, mg/dL                  | 98 (90, 107)    |
| HbA1C (%)                       | 5.8 (5.6, 6.7)  |
| Uric acid, mg/dL                | 5.8 (5.0, 7.0)  |
| eGFR, mL/min                    | 68 (54, 79)     |
| CRP, mg/dL                      | 0.3 (0.3, 0.75) |
| Log <sub>10</sub> BNP           | 1.73±0.70       |
| d-ROMs (U.CARR.) <sup>#</sup>   | 304±91          |

Data are expressed as means, medians or counts (%) as appropriate. ALT indicates alanine aminotransferase; AST, aspartate aminotransferase; CAVI, cardio-ankle vascular index; CRP, C-reactive protein; DCT, deceleration time; d-ROMs, derivatives of the reactive oxidative metabolites; E/E', index of LV diastolic dysfunction; EF, ejection fraction; eGFR, estimated glomerular filtration rate; HbA1C, hemoglobin A1C; HDL, high-density lipoprotein; LDL, low-density lipoprotein; Log<sub>10</sub>BNP, log-transformed brain natriuretic peptide (pg/mL); p-eNOS, phosphorylated endogenous nitric oxide synthase at Ser1177; WBC, white blood cells; ΔACh, percentage change in acetylcholine-induced p-eNOS; ΔINS, percentage change in insulin-induced p-eNOS; ΔVEGF, percentage change in VEGF-induced p-eNOS.

\*n=62.

<sup>†</sup>n=30.

<sup>‡</sup>n=47.

<sup>§</sup>n=46.

<sup>||</sup>n=54.

<sup>¶</sup>n=58.

<sup>#</sup>n=60.

eNOS.<sup>22–24</sup> In the Western blotting of human umbilical vein endothelial cells, p-eNOS Ser1177 was increased after augmented p-Akt Ser473 by human fresh serum.

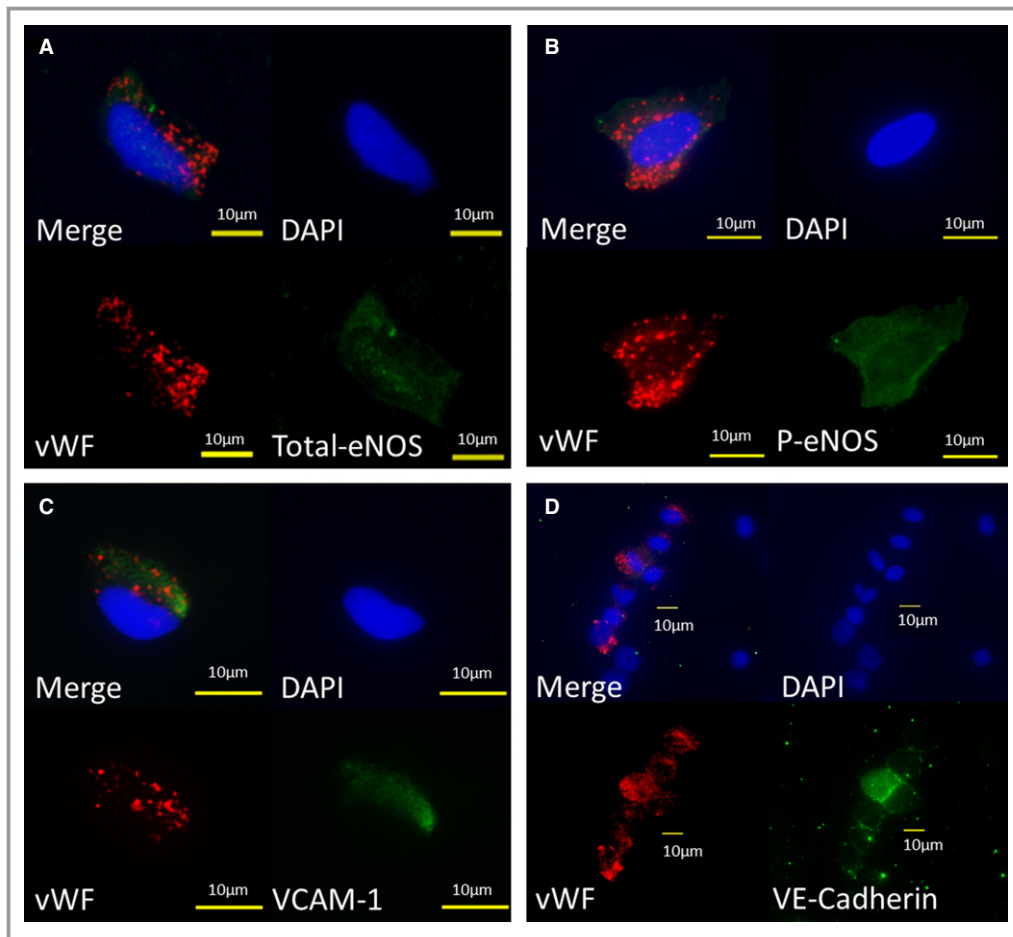


**Figure 2.** Representative images of the freshly isolated arterial endothelial cell. Red—von Willebrand Factor; Green—total eNOS (A), p-eNOS (B), VCAM-1 (C), vascular endothelial-cadherin (D); Blue—DAPI. DAPI indicates 4',6-diamidino-2-phenylindole stain; eNOS, endogenous nitric oxide synthase; p-eNOS, phosphorylated-eNOS at Ser1177; VCAM-1, vascular cell adhesion molecule-1; VE-cadherin, vascular endothelial cadherin; vWF, von Willebrand Factor.

This increase was eliminated by eNOS knockdown (Figures S5 and S6). Therefore, we subsequently cultured freshly isolated endothelial cells harvested from 18 patients with their serum. Figure 3 shows the endothelial cells collected from the same patient (Figure 3A and 3E: control, Figure 3B and 3F: serum-stimulation). The intensity of p-eNOS was dramatically increased by serum (Figure 3C and 3D). The p-eNOS Ser1177 intensity could be a positive control of the experiment.

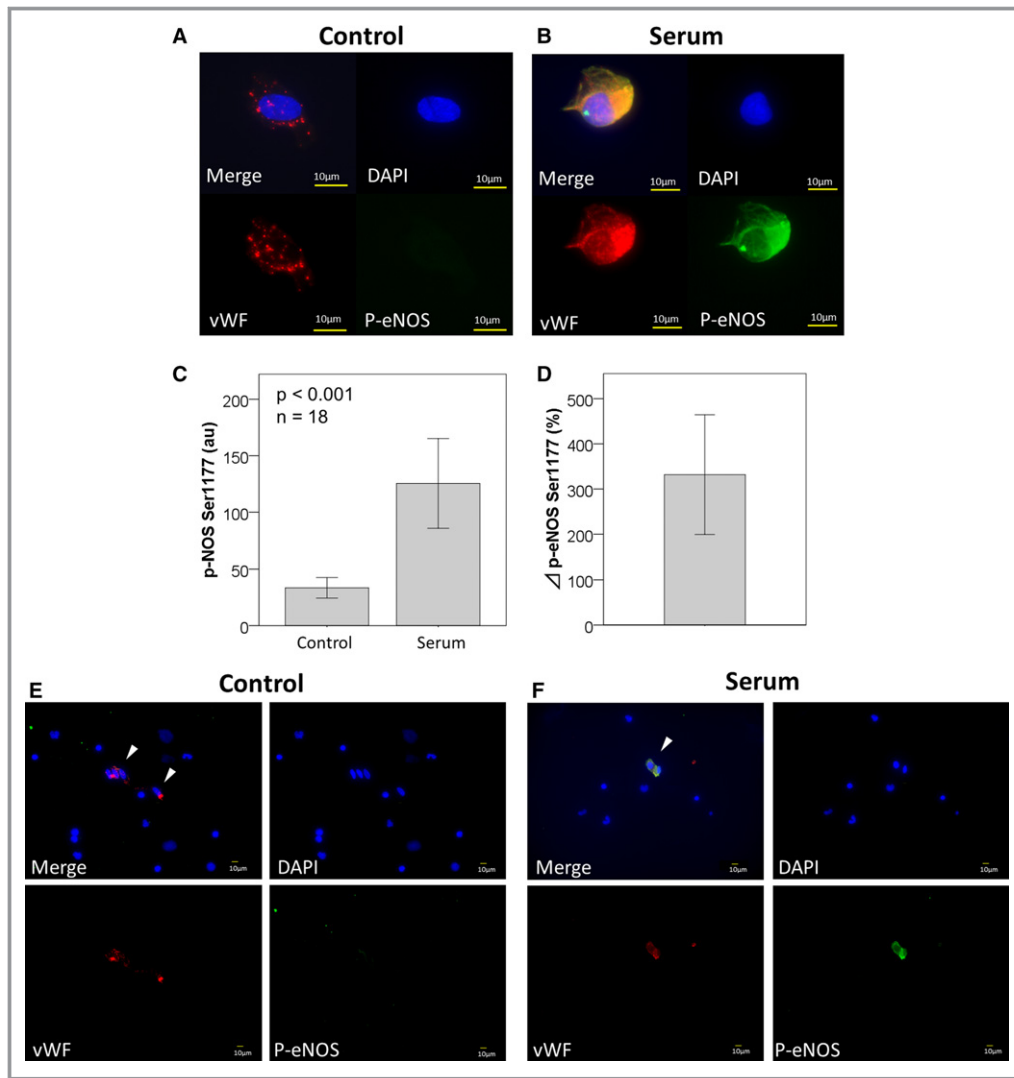
### Clinical Factors Associated With Basal Phosphorylation of eNOS at Ser1177

Table 3 shows the relationships between the clinical backgrounds of the patients and the immunofluorescence intensity of freshly isolated endothelial cells stained with p-eNOS antibody. The mean value of basal p-eNOS measured in arbitrary units (au) was  $41 \pm 22$  ( $n=69$ ). The quantitated

intensity was higher in patients with hyperlipidemia (hyperlipidemia,  $46 \pm 23$ ,  $n=43$ ; others,  $33 \pm 16$ ,  $n=26$ ;  $P=0.020$ ). In addition, the intensities in endothelial cells correlated positively with log-transformed brain natriuretic peptide BNP ( $\text{Log}_{10}\text{BNP}$ ) and negatively with levels of hemoglobin and hematocrit, suggesting the influence of heart failure.

### Clinical Factors Associated With eNOS Response to Insulin

The percentage change in insulin-induced p-eNOS ( $\Delta\text{INS}$ , %) was higher in men than in women (men,  $13 \pm 31$ ,  $n=47$ ; women,  $-12 \pm 25$ ,  $n=15$ ;  $P=0.005$ ).  $\Delta\text{INS}$  deteriorated with an increase in  $\text{Log}_{10}\text{BNP}$ ,  $E/E'$  and d-ROMs (Figure 4A through 4C) (Table 3).  $\Delta\text{INS}$  was positively correlated with eGFR (Figure 4D). These results suggested an association with heart failure, oxidative stress and renal function.



**Figure 3.** Serum-stimulation for a positive control. Freshly isolated endothelial cells harvested from a patient was incubated with serum-free medium as control (A) or serum obtained from the patient (B) for 30 minutes. The intensity of p-eNOS (arbitrary unit) was strongly increased by thrombin in the serum (control:  $33 \pm 20$ , serum  $125 \pm 80$ ,  $n=18$ ;  $P<0.001$ ) (C). The % increase of serum-stimulation was  $331 \pm 267$ , which was much higher than insulin, VEGF, acetylcholine (D). The images of low magnification (control: E; serum-stimulation: F) revealed that the intensity of p-eNOS was enhanced in only the vWF positive cells. The white arrows indicate the endothelial cells. DAPI indicates 4',6-diamidino-2-phenylindole stain; p-eNOS, phosphorylated-endogenous nitric oxide synthase at Ser1177; VEGF, vascular endothelial growth factor; vWF, von Willebrand Factor.

In addition,  $\Delta$ INS was not directly related to diabetes mellitus (DM), (DM,  $8 \pm 40$ ,  $n=20$ ; others,  $7 \pm 27$ ,  $n=42$ ;  $P=0.872$ ).  $\Delta$ INS did not correlate with HbA1C, fasting glucose level, fasting insulin level, homeostatic model assessment of insulin resistance (Figure 4E through 4H). However,  $\Delta$ INS was significantly decreased in diabetics using self-injections of insulin (insulin therapy,  $-29 \pm 18$ ,  $n=5$ ; others,  $10 \pm 30$ ,  $n=57$ ;  $P=0.006$ ). There were more women under insulin therapy than men (women,  $n=4/15$  [27%]; men,  $n=1/47$  [2%];  $P=0.010$ ). In a subgroup of type-2 DM patients,  $\Delta$ INS was significantly reduced in patients with CAD compared with those without it (CAD,  $-3 \pm 39$ ,  $n=14$ ; non-CAD,  $33 \pm 34$ ,  $n=6$ ;  $P=0.012$ ).

### Clinical Factors Associated With eNOS Response to VEGF, and Acetylcholine

The percentage change in VEGF-induced p-eNOS ( $\Delta$ VEGF, %) was decreased in current smokers (current smoker,  $-16 \pm 22$ ,  $n=12$ ; others,  $10 \pm 31$ ,  $n=18$ ;  $P=0.020$ ). Furthermore, it was reduced in patients using furosemide (furosemide,  $-21 \pm 27$ ,  $n=7$ ; others,  $6 \pm 29$ ,  $n=23$ ;  $P=0.037$ ).  $\Delta$ VEGF correlated negatively with d-ROMs (Table 3, Figure 5A). Although  $\Delta$ VEGF was not significantly associated with  $\text{Log}_{10}$ BNP in this study, d-ROMs were moderately associated with  $\text{Log}_{10}$ BNP ( $r=0.516$ ,  $n=60$ ,  $P<0.001$ ).  $\Delta$ VEGF also correlated with serum levels of

**Table 3.** Relationship Between p-eNOS and Clinical Factors

| No. of Patients                 | Basal p-eNOS (69) |         | ΔINS (62) |         | ΔVEGF (30) |         | ΔACh (47) |         |
|---------------------------------|-------------------|---------|-----------|---------|------------|---------|-----------|---------|
|                                 | ρ/r               | P Value | ρ/r       | P Value | ρ/r        | P Value | ρ/r       | P Value |
| Age, y                          | 0.166             | 0.172   | −0.170    | 0.187   | 0.062      | 0.746   | −0.151    | 0.312   |
| BMI, kg/m <sup>2</sup>          | −0.175            | 0.149   | 0.145     | 0.260   | −0.019     | 0.919   | 0.146     | 0.327   |
| WBC, /μL                        | −0.042            | 0.734   | 0.167     | 0.193   | −0.007     | 0.971   | 0.189     | 0.204   |
| Hemoglobin, g/dL                | −0.237            | 0.050*  | 0.167     | 0.195   | 0.110      | 0.562   | 0.005     | 0.975   |
| Hematocrit, %                   | −0.294            | 0.014*  | 0.037     | 0.773   | 0.073      | 0.701   | −0.012    | 0.936   |
| Platelets, ×10 <sup>4</sup> /μL | −0.131            | 0.282   | 0.045     | 0.726   | 0.167      | 0.377   | 0.090     | 0.547   |
| AST, IU/L                       | 0.076             | 0.535   | −0.107    | 0.410   | −0.447     | 0.013*  | 0.208     | 0.162   |
| ALT, IU/L                       | −0.044            | 0.720   | −0.075    | 0.563   | −0.549     | 0.002*  | 0.050     | 0.740   |
| LDL cholesterol, mg/dL          | 0.035             | 0.773   | −0.013    | 0.198   | 0.250      | 0.182   | −0.190    | 0.201   |
| Triglyceride, mg/dL             | −0.030            | 0.807   | 0.083     | 0.522   | 0.338      | 0.068   | 0.002     | 0.991   |
| HDL cholesterol, mg/dL          | −0.170            | 0.163   | −0.067    | 0.604   | 0.063      | 0.740   | −0.054    | 0.718   |
| Glucose, mg/dL                  | −0.220            | 0.070   | 0.081     | 0.531   | −0.109     | 0.568   | −0.048    | 0.750   |
| HbA1C, %                        | 0.042             | 0.732   | −0.100    | 0.439   | 0.000      | 0.998   | −0.139    | 0.352   |
| Uric acid, mg/dL                | 0.194             | 0.111   | −0.005    | 0.967   | −0.145     | 0.443   | −0.144    | 0.336   |
| eGFR, mL/min                    | −0.190            | 0.119   | 0.294     | 0.020*  | 0.196      | 0.298   | 0.345     | 0.018*  |
| CRP, mg/dL                      | 0.175             | 0.151   | 0.011     | 0.932   | −0.064     | 0.735   | −0.117    | 0.432   |
| Log <sub>10</sub> BNP           | 0.288             | 0.016*  | −0.266    | 0.037*  | −0.305     | 0.101   | −0.183    | 0.217   |
| d-ROMs (U.CARR.) <sup>†</sup>   | 0.094             | 0.475   | −0.348    | 0.011*  | −0.416     | 0.022*  | −0.110    | 0.507   |
| E/E' <sup>‡</sup>               | 0.039             | 0.778   | −0.374    | 0.008*  | −0.180     | 0.400   | −0.191    | 0.245   |
| DCT, ms <sup>§</sup>            | 0.065             | 0.626   | −0.246    | 0.076   | −0.331     | 0.091   | −0.039    | 0.808   |
| EF, % <sup>  </sup>             | −0.205            | 0.116   | −0.076    | 0.581   | −0.200     | 0.308   | −0.060    | 0.703   |

ALT indicates alanine aminotransferase; AST, aspartate aminotransferase; BMI, body mass index; CRP, C-reactive protein; DCT, deceleration time; d-ROMs, derivatives of the reactive oxidative metabolites; E/E', index of LV diastolic dysfunction; EF, ejection fraction; eGFR, estimated glomerular filtration rate; HbA1C, hemoglobin A1C; HDL, high-density lipoprotein; LDL, low-density lipoprotein; Log<sub>10</sub>BNP, log-transformed brain natriuretic peptide (pg/mL); p-eNOS, phosphorylated endogenous nitric oxide synthase at Ser1177; WBC, white blood cells; ΔACh, percentage change in ACh-induced p-eNOS; ΔINS, percentage change in insulin-induced p-eNOS; ΔVEGF, percentage change in VEGF-induced p-eNOS.

\* $p < 0.05$ .

Numbers of basal p-eNOS/ΔINS/ΔVEGF/ΔACh=†60/53/30/39, ‡54/49/24/39, §58/53/27/42, ||60/55/28/43.

aspartate aminotransferase and alanine aminotransferase (Figure 5B and 5C).

In contrast, the percentage change in acetylcholine - induced p-eNOS (ΔACh, %) increased with a decrease in eGFR (Figure 5D). ΔACh was higher in patients with chronic kidney disease defined as eGFR <60 mL/min (chronic kidney disease,  $-8 \pm 25$ ,  $n=18$ ; non-chronic kidney disease,  $16 \pm 43$ ,  $n=29$ ;  $P=0.037$ ).

### Representative Images of eNOS Activation and CAVI

The representative images of the 2 cases with high and low CAVI are shown in Figure 6. In the case of low CAVI, the basal p-eNOS intensity was low while the insulin-induced p-eNOS intensity was high (Figure 6A). However, the difference was reduced in patients with high CAVI by both the

elevation of basal intensity and reduced response to insulin (Figure 6B).

### Regression Analyses for CAVI

Univariate analysis showed that ΔINS was inversely associated with CAVI (Table 4, Figure 7). In multivariate regression analysis, the crude model (model 1) showed that the relationship between ΔINS and CAVI was not significant. However, the traditional stepwise regression model (model 2) and the adaptive Lasso regression model (model 3) showed that ΔINS was independently associated with CAVI (Figure S7).

### Discussion

This cross-sectional study using a novel method had 2 major findings. First, ΔINS inversely correlated with oxidative stress,



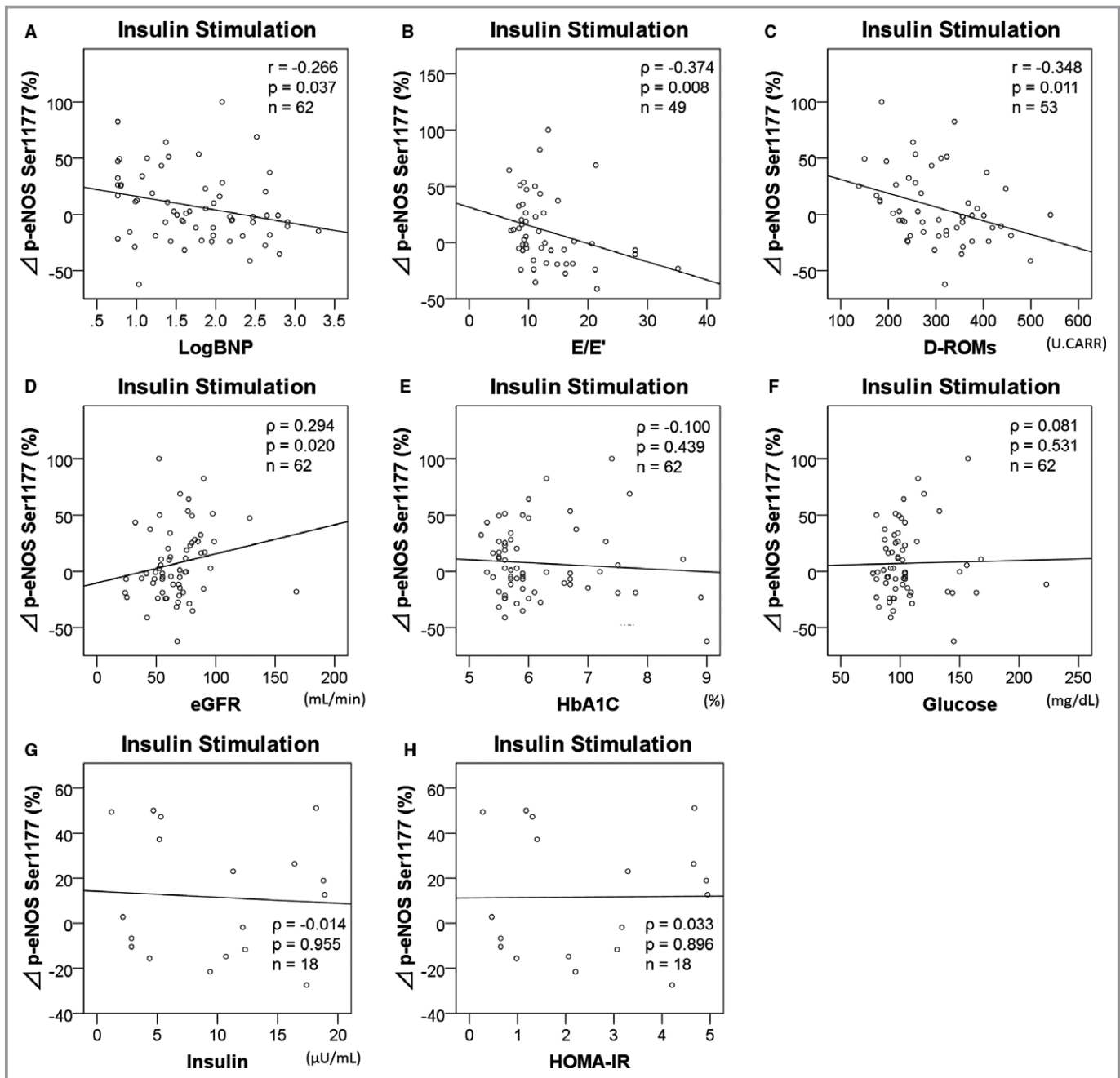


**Figure 4.** Correlations of insulin-induced increase of p-eNOS Ser1177 with confounding factors. Freshly isolated arterial endothelial cells were cultured in medium for 30 minutes before fixing with or without insulin (100 nmol/L, 30 minutes). The percentage increase in p-eNOS by insulin from the basal p-eNOS correlated with Log<sub>10</sub>BNP (A), E/E' (B), d-ROMs (C) and eGFR (D), but did not correlate with HbA1C (E), fasting glucose level (F), fasting insulin level (G), HOMA-IR (H). d-ROMs indicates derivatives of the reactive oxidative metabolites; E/E', index of LV diastolic dysfunction; eGFR, estimated glomerular filtration rate; HbA1C, hemoglobin A1C; HOMA-IR, homeostatic model assessment of insulin resistance; Log<sub>10</sub>BNP, log-transformed brain natriuretic peptide (pg/mL); p-eNOS, phosphorylated-endothelial nitric oxide synthase at Ser1177.

Log<sub>10</sub>BNP and E/E', an index of LV diastolic dysfunction on Doppler echocardiography. Second,  $\Delta$ INS was independently associated with CAVI. These relationships are reasonable because CAVI is closely related to E/E'.<sup>25</sup> Thus, endothelial IR was associated with arterial stiffness, LV diastolic

dysfunction, and heart failure in this study. However, arterial stiffness and heart failure might induce endothelial IR (Figure 8).<sup>26,27</sup>

Heart failure is a condition of high oxidative stress and the increased secretion of proinflammatory cytokines. Therefore,

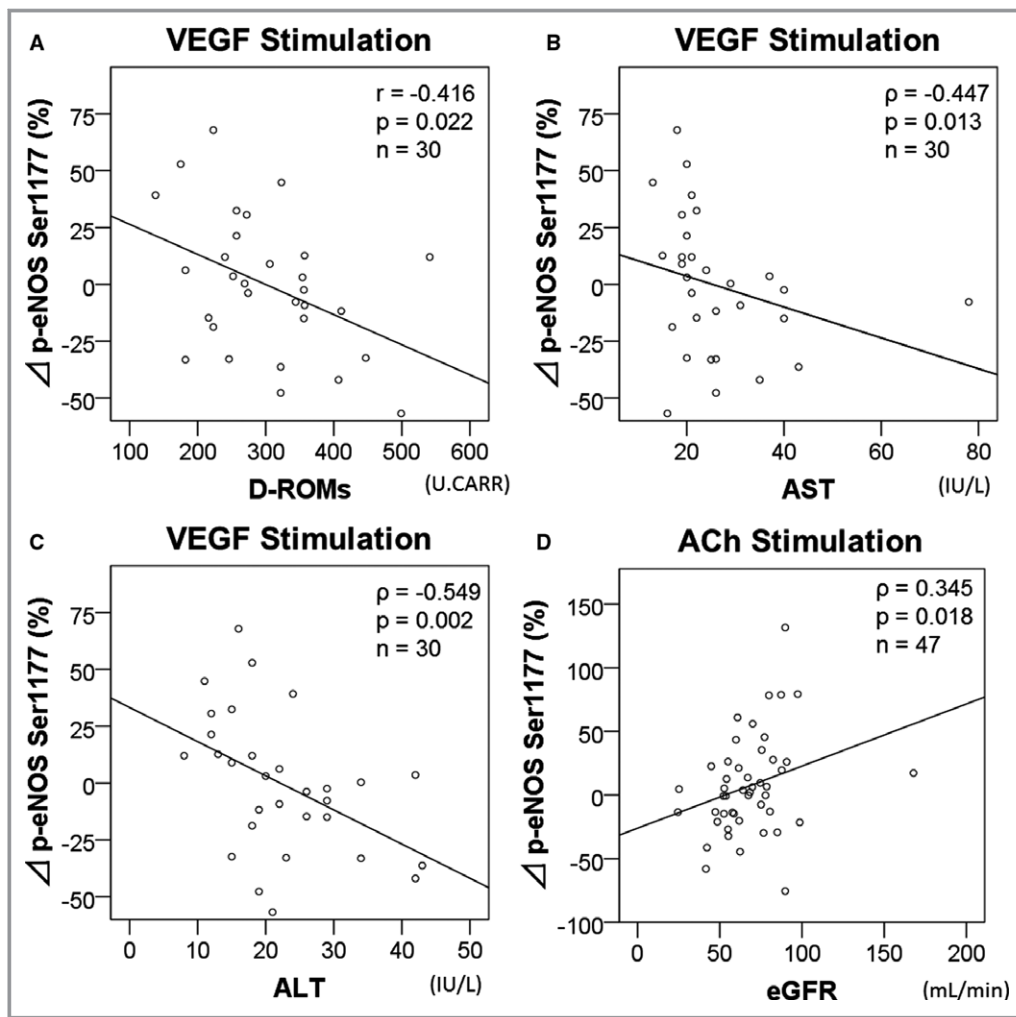


**Figure 5.** Correlations of VEGF, acetylcholine-stimulated increase of p-eNOS Ser1177 with confounding factors. Freshly acetylcholine arterial endothelial cells were cultured in medium with or without VEGF (20 ng/mL, 30 minutes), or acetylcholine (1  $\mu$ mol/L, 15 minutes). The percentage increase in p-eNOS by VEGF from the basal p-eNOS correlated with d-ROMs (A), AST (B) and ALT (C). The percentage increase of acetylcholine-induced p-eNOS correlated with eGFR (D). ALT indicates alanine aminotransferase; AST, aspartate aminotransferase; d-ROMs, derivatives of the reactive oxidative metabolites; eGFR, estimated glomerular filtration rate; p-eNOS, phospho-endogenous nitric oxide synthase at Ser1177; VEGF, vascular endothelial growth factor.

it is reasonable to think that signal transduction in the IRS-1/PI3K/Akt/eNOS pathway could be impaired in heart failure.<sup>26</sup> It was previously reported that insulin signaling can be impaired by non-diabetic causes including oxidized low density lipoprotein cholesterol,<sup>28</sup> angiotensin II,<sup>29,30</sup> vasopressin,<sup>31</sup> TNF- $\alpha$ ,<sup>32</sup> leptin,<sup>33,34</sup> uric acid,<sup>35</sup> various hormones,<sup>36</sup> and chronic kidney disease.<sup>37</sup> Our results are concordant with clinical studies that have reported that endothelial dysfunction is accompanied with chronic congestive heart failure<sup>38–40</sup> and increased mortality from heart failure.<sup>41</sup>

Arterial stiffness increases pulse wave reflection and causes LV diastolic dysfunction. Therefore, it is considered

an exacerbating factor in heart failure.<sup>42,43</sup> The primary cause of arterial stiffness is a change in medial structural components.<sup>44</sup> Matrix metalloproteinases promote overproduction of abnormal collagen and degradation of elastin in the extracellular matrix.<sup>45</sup> Moreover, an accumulation of advanced glycation end products, calcium deposition, neurohormonal factors, and sympathetic nerve activation also play roles in development of arterial stiffness. In addition to the structural changes, endothelial dysfunction provokes vasomotor dysregulation and vascular stiffening.<sup>46–48</sup> Therefore, endothelial IR, which indicates the dysregulation of IRS-1/PI3-kinase/Akt/eNOS signaling, could be involved in the pathogenesis of arterial stiffness.

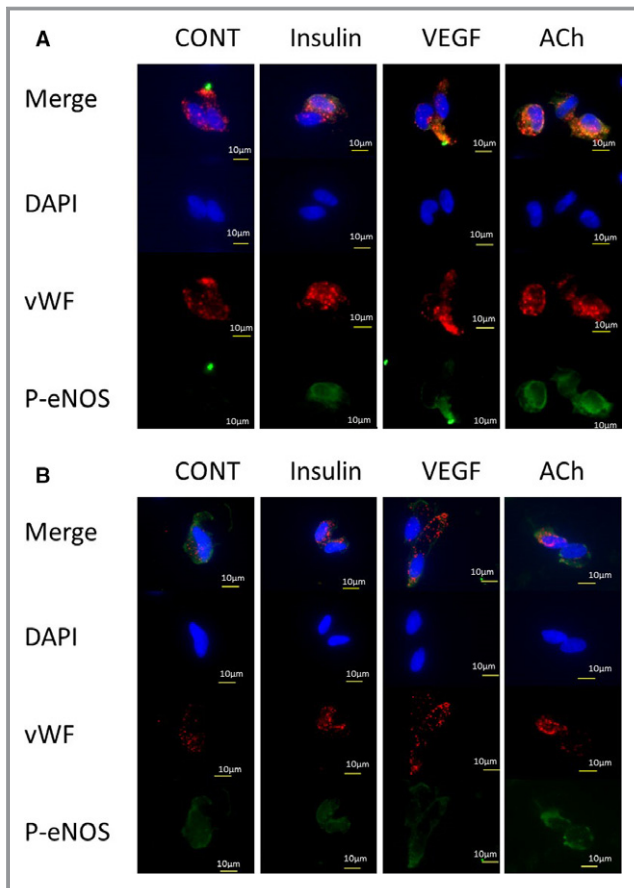


**Figure 6.** Images of p-eNOS Ser1177 in patients with low and high CAVI scores. **A**, The images are from a 57-year-old non-CAD man who had a history of smoking and obesity only (bone mass index: 27.1). CAVI was 7.77. Among laboratory data, BNP (25.4 pg/mL) and eGFR (97.4 mL/min) were within normal range. The basal p-eNOS intensity was at low level (CONT). The intensity was increased by stimulation with insulin (+51%), VEGF (+45%), and acetylcholine (+79%). **B**, The images from a 75-year-old man with severe CAD and low cardiac function (ejection fraction 20%). He had diabetes mellitus, hypertension, hyperlipidemia, and was a current smoker. BNP was 1981.7 pg/mL ( $\text{Log}_{10}\text{BNP}$ : 3.30); however, renal function was within normal range (eGFR 69.8 mL/min). CAVI score was 10.11. The basal p-eNOS was already enhanced (CONT), and the responses to stimuli were reduced. These resulted in decreases in the percentage changes induced by insulin (−1.6%) and VEGF (−27%). However, the acetylcholine-induced p-eNOS intensity was not reduced (+11%). Red—von Willebrand Factor; Green—p-eNOS; Blue—DAPI. BMI indicates body mass index; BNP, brain natriuretic peptide (pg/mL); CAD, coronary artery disease; CAVI, cardio-ankle vascular index; CONT, control; DAPI indicates 4',6-diamidino-2-phenylindole stain; eGFR, estimated glomerular filtration rate; p-eNOS, phosphorylated endogenous nitric oxide synthase at Ser1177; VEGF, vascular endothelial growth factor; vWF, von Willebrand Factor.

Surprisingly, the patients with type-2 DM in this study did not always have endothelial IR, although most previous studies have explored the mechanisms of endothelial IR in

subjects with obesity or type-2 DM. Because most patients had severe atherosclerotic disease and/or heart failure, the difference attributable to diabetes mellitus was difficult to be elucidated. However, all type-2 DM patients under insulin therapy had decreased eNOS response to insulin. There were more women under insulin therapy than men. We think that was the main reason for the sex difference of  $\Delta\text{INS}$  in our study. Additionally, a sub-analysis of type-2 DM patients revealed that insulin-induced eNOS activation was significantly lower in diabetics who had CAD than those who did not. Thus, the duration, severity, and treatment of type-2 DM might influence endothelial IR and further investigation is needed.

We tested the response of eNOS to stimuli other than insulin. VEGF is an important regulator of endothelial healing and growth and angiogenesis after vascular injury. VEGF mediates the release of NO via the IRS-1/PI3-kinase/Akt/eNOS pathway in the process.<sup>49</sup>  $\Delta\text{VEGF}$  was attenuated in smokers in our results. This is concordant with a previous study showing that cigarette smoke impairs VEGF-dependent activation of the Akt/eNOS/NO pathway in human umbilical vein endothelial cells.<sup>50</sup> Furthermore,  $\Delta\text{VEGF}$  was associated with d-ROMs similarly to  $\Delta\text{INS}$ . We previously showed an association between d-ROMs, serum levels of BNP, and high-sensitivity C-reactive protein.<sup>51</sup> Because oxidative stress is a common mediator of atherosclerosis, heart failure, and inflammation, it is understandable that high-oxidative stress can decrease  $\Delta\text{INS}$  and  $\Delta\text{VEGF}$ .

In contrast, the clinical factors associated with  $\Delta\text{ACh}$  did not match those of  $\Delta\text{INS}$  and  $\Delta\text{VEGF}$ . Various cascades in acetylcholine-induced phosphorylation of eNOS have been previously reported.<sup>52–56</sup> Acetylcholine induces rapid tyrosine phosphorylation and the activation of Janus kinase 2 signaling, which is upstream of the IRS-1/PI 3-kinase/Akt/eNOS pathway.<sup>56</sup> This is an additional mechanism of acetylcholine-induced eNOS activation transferred to a calcium-dependent activation.<sup>57,58</sup> However, our sample size was too small to allow an evaluation of other signaling molecules underlying the activation of acetylcholine-induced eNOS. Thus, further investigation is required to clarify the differences between  $\Delta\text{INS}$ ,  $\Delta\text{VEGF}$ , and  $\Delta\text{ACh}$ .

To our knowledge, this is the first study to investigate freshly isolated arterial endothelial cells collected from a radial catheter sheath used for coronary angiography. Because commercialized human aortic endothelial cells and retrieved endothelial cells from animal tissues need stabilization in culture medium for a long time before experimental processes, we think that our non-invasive method could be advantageous for evaluating the phenotypes of cardiovascular disease, including arterial stiffness. Furthermore, a future aim is to find a way to restore endothelial function and inhibit the progression of arterial stiffness.

**Table 4.** Regression Analysis for CAVI

| No. of Patients                      | Univariate (46) |                     | Multivariate (42) |         |         |         |         |         |
|--------------------------------------|-----------------|---------------------|-------------------|---------|---------|---------|---------|---------|
|                                      |                 |                     | Model 1           |         | Model 2 |         | Model 3 |         |
|                                      | $\beta$         | P Value             | $\beta$           | P Value | $\beta$ | P Value | $\beta$ | P Value |
| $\Delta$ INS, %                      | -0.317          | 0.041* <sup>†</sup> | -0.291            | 0.059   | -0.332  | 0.017*  | -0.293  | 0.021*  |
| Age, y                               | 0.567           | <0.001*             | 0.484             | 0.004*  | 0.475   | <0.001* | 0.489   | <0.001* |
| Sex, man 1, woman 0                  | 0.084           | 0.579               | 0.218             | 0.136   | 0.263   | 0.048*  | 0.213   | 0.025*  |
| Hypertension, yes 1, no 0            | 0.098           | 0.516               | 0.046             | 0.757   |         |         |         |         |
| Hyperlipidemia, yes 1, no 0          | 0.127           | 0.400               | -0.047            | 0.757   |         |         |         |         |
| Diabetes mellitus, yes 1, no 0       | 0.095           | 0.528               | 0.184             | 0.192   |         |         | 0.179   | 0.126   |
| Current smoking, yes 1, no 0         | -0.116          | 0.444               | 0.025             | 0.882   |         |         |         |         |
| Hemoglobin, g/dL                     | -0.376          | 0.010*              | -0.048            | 0.862   |         |         |         |         |
| Hematocrit, %                        | -0.313          | 0.034*              | -0.160            | 0.551   | -0.255  | 0.038*  | -0.209  | 0.010*  |
| Platelets, $\times 10^4/\mu\text{L}$ | -0.308          | 0.038*              | -0.198            | 0.156   |         |         | -0.171  | 0.099   |
| eGFR, mL/min                         | -0.375          | 0.010*              | -0.032            | 0.841   |         |         |         |         |
| d-ROMs (U.CARR.)                     | 0.331           | 0.034* <sup>‡</sup> |                   |         |         |         |         |         |

This table displays the 3 models including  $\Delta$ INS in multivariate regression model analysis. The adjusted  $R^2$  was 0.405,  $P=0.003$  for model 1; 0.509,  $P<0.001$  for model 2; 0.560,  $P<0.001$  for model 3, respectively. The original prediction formula and the solution path for model 3 were also shown in supplemental material. d-ROMs indicates derivatives of the reactive oxidative metabolites; eGFR, estimated glomerular filtration rate;  $\Delta$ INS, percentage change in insulin-induced p-eNOS at Ser1177.

\* $p<0.05$ .

<sup>†</sup> $n=42$ .

<sup>‡</sup> $n=41$ .

Many patients undergo repetitive coronary angiographies; thus this method is applicable for these patients so that the effects of drugs, nutrition, and lifestyle interventions can be seen.

This study had several limitations. First, the number of patients was too small to evaluate all underlying factors

and drug effects that affect eNOS activity. The relatively small sample size for the CAVI analysis is concerning when attempting a multiple regression with a potentially large number of predictors. Therefore, we confirmed the association of  $\Delta$ INS with CAVI by different modeling strategies. However, more samples are needed for accuracy. Second, this observational study did not have a control group of healthy participants because all participants had to have a reason to undergo coronary angiography. Third, we assessed endothelial IR with the percentage changes in p-eNOS; however, total eNOS was not evaluated. There were possibilities that the variability of staining intensity could not be completely excluded even though control slides were used, and excessive standardization such as dividing p-eNOS by total eNOS could diminish the accuracy. Accordingly, we thought that measurements of percentage change could be more reliable markers, because the effect of total eNOS and the variability of staining intensity were eliminated in the formula. In addition, the Western blots of the phosphorylated and total eNOS of the endothelial cells with or without insulin treatment are more reliable than immunofluorescence. Using some commercialized devices, Western blotting may be available from the limited number of the endothelial cells obtained from catheter sheaths. Thus, we need to confirm the results by multiple methods in the future.

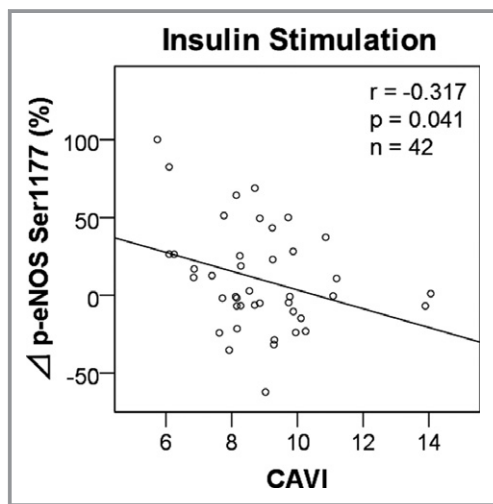


**Figure 7.** Correlations between p-eNOS Ser1177 and CAVI. CAVI score correlated with percentage change of insulin-induced p-eNOS at Ser1177. CAVI indicates cardio-ankle vascular index.

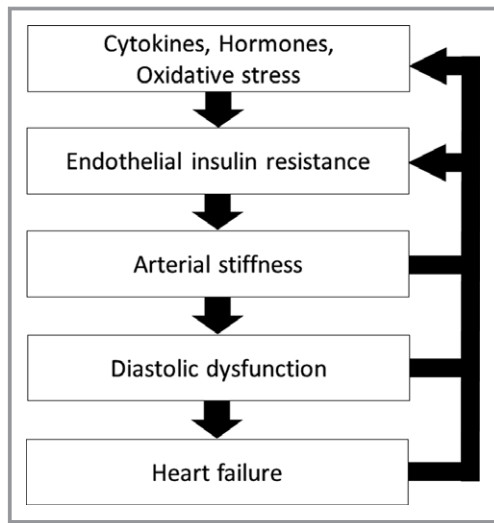


**Figure 8.** Overview of the relationship between endothelial insulin resistance and heart failure. The flowchart shows our view, which is that endothelial insulin resistance is associated with arterial stiffness and heart failure.

## Conclusion

In conclusion, our findings suggested endothelial IR is associated with oxidative stress, LV diastolic dysfunction, arterial stiffness, and heart failure. This molecular biological assessment of freshly isolated arterial endothelial cells taken from radial sheaths may help us understand endothelial IR in clinical practice.

## Acknowledgments

We would like to thank Atsushi Sato, Toyokazu, Kimura, Shunpei Horii, Ayumu Ohsaki, Kei Ito, Kazuki Kagami, Risako Yasuda, Yasunaga Shiraishi, Takayuki Namba, Yuji Nagatomo, and Hirota Yada of the Department of Cardiology, National Defense Medical College for their cooperation in collecting the specimens during coronary angiographies and for their support with the experiments.

## Sources of Funding

This work was supported by a Grant-in-aid for Scientific Research from the Ministry of Education, Science, and Culture of Japan (to Masaki) (17K09565) and a grant (to Adachi) from the Ministry of Defense.

## Disclosures

None.

## References

1. Riehle C, Abel ED. Insulin signaling and heart failure. *Circ Res*. 2016; 118:1151–1169.

- Fulton DJR. Mechanisms of vascular insulin resistance. A substitute Akt? *Circ Res*. 2009;104:1035–1037.
- Muniyappa R, Sowers JR. Role of insulin resistance in endothelial dysfunction. *Rev Endocr Metab Disord*. 2013;14:5–12.
- Fulton D, Gratton JP, McCabe TJ, Fontana J, Fujio Y, Walsh K, Franke TF, Papapetropoulos A, Sessa WC. Regulation of endothelium-derived nitric oxide production by the protein kinase Akt. *Nature*. 1999;399:597–601.
- Montagnani M, Chen H, Barr VA, Quon MJ. Insulin-stimulated activation of eNOS is independent of  $Ca^{2+}$  but requires phosphorylation by Akt at Ser (1179). *J Biol Chem*. 2001;276:30392–30398.
- Zhang QJ, McMillin SL, Tanner JM, Palionyte M, Abel ED, Symons JD. Endothelial nitric oxide synthase phosphorylation in treadmill-running mice: role of vascular signalling kinases. *J Physiol*. 2009;587:3911–3920.
- Gélinas DS, Bernatchez PN, Rollin S, Bazan NG, Sirois MG. Immediate and delayed VEGF-mediated NO synthesis in endothelial cells: role of PI3K, PKC and PLC pathways. *Br J Pharmacol*. 2002;137:1021–1030.
- Carreau A, Kieda C, Grillon C. Nitric oxide modulates the expression of endothelial cell adhesion molecules involved in angiogenesis and leukocyte recruitment. *Exp Cell Res*. 2011;317:29–41.
- Apostoli GL, Solomon A, Smallwood MJ, Winyard PG, Emerson M. Role of inorganic nitrate and nitrite in driving nitric oxide-cGMP-mediated inhibition of platelet aggregation in vitro and in vivo. *J Thromb Haemost*. 2014;12:1880–1889.
- Qiu J, Zheng Y, Hu J, Liao D, Gregersen H, Deng X, Fan Y, Wang G. Biomechanical regulation of vascular smooth muscle cell functions: from in vitro to in vivo understanding. *J R Soc Interface*. 2013;11:20130852.
- Tabit CE, Shenouda SM, Holbrook M, Fetterman JL, Kiani S, Frame AA, Kluge MA, Held A, Dohadwala MM, Gokce N, Farb MG, Rosenzweig J, Ruderman N, Vita JA, Hamburg NM. Protein kinase C- $\beta$  contributes to impaired endothelial insulin signaling in humans with diabetes mellitus. *Circulation*. 2013;127:86–95.
- Bretón-Romero R, Feng B, Holbrook M, Farb MG, Fetterman JL, Linder EA, Berk BD, Masaki N, Weisbrod RM, Inagaki E, Gokce N, Fuster JJ, Walsh K, Hamburg NM. Endothelial dysfunction in human diabetes is mediated by Wnt5a-JNK signaling. *Arterioscler Thromb Vasc Biol*. 2016;36:561–569.
- Spoto B, Pisano A, Zoccali C. Insulin resistance in chronic kidney disease: a systematic review. *Am J Physiol Renal Physiol*. 2016;311:F1087–F1108.
- Shirai K, Hiruta N, Song M, Kurosu T, Suzuki J, Tomaru T, Miyashita Y, Saiki A, Takahashi M, Suzuki K, Takata M. Cardio-ankle vascular index (CAVI) as a novel indicator of arterial stiffness: theory, evidence and perspectives. *J Atheroscler Thromb*. 2011;18:924–938.
- Imai E, Horio M, Nitta K, Yamagata K, Iseki K, Hara S, Ura N, Kiyohara Y, Hirakata H, Watanabe T, Moriyama T, Ando Y, Inaguma D, Narita I, Iso H, Wakai K, Yasuda Y, Tsukamoto Y, Ito S, Makino H, Hishida A, Matsuo S. Estimation of glomerular filtration rate by the MDRD study equation modified for Japanese patients with chronic kidney disease. *Clin Exp Nephrol*. 2006;11:41–50.
- Alberti A, Bolognini L, Macciantelli D, Caratelli M. The radical cation of N, N-diethylpara-phenylendiamine: a possible indicator of oxidative stress in biological samples. *Res Chem Intermed*. 2000;26:253–267.
- Cesarone MR, Belcaro G, Carratelli M, Cornelli U, De Sanctis MT, Incandela L, Barsotti A, Terranova R, Nicolaidis A. A simple test to monitor oxidative stress. *Int Angiol*. 1999;18:127–130.
- Haffner SM, Miettinen H, Stern MP. The homeostasis model in the San Antonio Heart Study. *Diabetes Care*. 1997;20:1087–1092.
- Bonarjee VVS. Arterial stiffness: a prognostic marker in coronary heart disease. available methods and clinical application. *Front Cardiovasc Med*. 2018;5:64.
- Gohbara M, Iwashita N, Sano Y, Akiyama E, Maejima N, Tsukahara K, Hibi K, Kosuge M, Ebina T, Umemura S, Kimura K. Clinical impact of the cardio-ankle vascular index for predicting cardiovascular events after acute coronary syndrome. *Circ J*. 2016;80:1420–1426.
- Harrell F. *Regression Modeling Strategies*. Cham, Switzerland: Springer; 2015:63–102.
- Thors B, Halldórsson H, Jónsdóttir G, Thorgeirsson G. Mechanism of thrombin mediated eNOS phosphorylation in endothelial cells is dependent on ATP levels after stimulation. *Biochim Biophys Acta*. 2008;1783:1893–1902.
- Motley ED, Eguchi K, Patterson MM, Palmer PD, Suzuki H, Eguchi S. Mechanism of endothelial nitric oxide synthase phosphorylation and activation by thrombin. *Hypertension*. 2007;49:577–583.
- Touyz RM. Regulation of endothelial nitric oxide synthase by thrombin. *Hypertension*. 2007;49:429–431.
- Namba T, Masaki N, Matsuo Y, Sato A, Kimura T, Horii S, Yasuda R, Yada H, Kawamura A, Takase B, Adachi T. Arterial stiffness is significantly associated



- with left ventricular diastolic dysfunction in patients with cardiovascular disease. *Int Heart J*. 2016;57:729–735.
26. Arora AR, Mandavia CH, Sowers JR. Insulin resistance and heart failure: molecular mechanisms. *Heart Fail Clin*. 2012;8:609–617.
  27. Mozos I, Malainer C, Horbańczuk J, Gug C, Stoian D, Luca CT, Atanasov AG. Inflammatory markers for arterial stiffness in cardiovascular diseases. *Front Immunol*. 2017;8:1058.
  28. Clavreul N, Bachschmid MM, Hou X, Shi C, Idrizovic A, Ido Y, Pimentel D, Cohen RA. S-glutathiolation of p21ras by peroxynitrite mediates endothelial insulin resistance caused by oxidized low-density lipoprotein. *Arterioscler Thromb Vasc Biol*. 2006;26:2454–2461.
  29. Andreozzi F, Laratta E, Sciacqua A, Perticone F, Sesti G. Angiotensin II impairs the insulin signaling pathway promoting production of nitric oxide by inducing phosphorylation of insulin receptor substrate-1 on Ser312 and Ser616 in human umbilical vein endothelial cells. *Circ Res*. 2004;94:1211–1218.
  30. Arora AR, Demarco VG, Jia G, Sun Z, Nistala R, Meininger GA, Sowers JR. The role of tissue renin-angiotensin-aldosterone system in the development of endothelial dysfunction and arterial stiffness. *Front Endocrinol (Lausanne)*. 2013;4:161.
  31. Kaufmann JE, Iezzi M, Vischer UM. Desmopressin (DDAVP) induces NO production in human endothelial cells via V2 receptor- and cAMP-mediated signaling. *J Thromb Haemost*. 2003;1:821–828.
  32. da Costa RM, Neves KB, Mestriner FL, Louzada-Junior P, Bruder-Nascimento T, Tostes RC. TNF- $\alpha$  induces vascular insulin resistance via positive modulation of PTEN and decreased Akt/eNOS/NO signaling in high fat diet-fed mice. *Cardiovasc Diabetol*. 2016;15:119.
  33. Ding N, Liu B, Song J, Bao S, Zhen J, Lv Z, Wang R. Leptin promotes endothelial dysfunction in chronic kidney disease through AKT/GSK3 $\beta$  and  $\beta$ -catenin signals. *Biochem Biophys Res Commun*. 2016;480:544–551.
  34. Vecchione C, Maffei A, Colella S, Aretini A, Poulet R, Frati G, Gentile MT, Fratta L, Trimarco V, Trimarco B, Lembo G. Leptin effect on endothelial nitric oxide is mediated through Akt-endothelial nitric oxide synthase phosphorylation pathway. *Diabetes*. 2002;51:168–173.
  35. Choi YJ, Yoon Y, Lee KY, Hien TT, Kang KW, Kim KC, Lee J, Lee MY, Lee SM, Kang DH, Lee BH. Uric acid induces endothelial dysfunction by vascular insulin resistance associated with the impairment of nitric oxide synthesis. *FASEB J*. 2014;28:3197–3204.
  36. Duckles SUE P. Hormonal modulation of endothelial NO production. *Pflugers Arch*. 2010;459:841–851.
  37. Zhou QG, Fu XJ, Xu GY, Cao W, Liu HF, Nie J, Liang M, Hou FF. Vascular insulin resistance related to endoplasmic reticulum stress in aortas from a rat model of chronic kidney disease. *Am J Physiol Heart Circ Physiol*. 2012;303:H1154–H1165.
  38. Katz SD, Biasucci L, Sabba C, Strom JA, Jondeau G, Galvao M, Solomon S, Nikolic SD, Forman R, LeJemtel TH. Impaired endothelium-mediated vasodilation in the peripheral vasculature of patients with congestive heart failure. *J Am Coll Cardiol*. 1992;19:918–925.
  39. Drexler H, Hayoz D, Munzel T, Hornig B, Just H, Brunner HR, Zelis R. Endothelial function in chronic congestive heart failure. *Am J Cardiol*. 1992;69:1596–1601.
  40. Marti CN, Gheorghiane M, Kalogeropoulos AP, Georgiopoulou VV, Quyyumi AA, Butler J. Endothelial dysfunction, arterial stiffness, and heart failure. *J Am Coll Cardiol*. 2012;60:1455–1469.
  41. Katz SD, Hryniewicz K, Hriljac I, Balidemaj K, Dimayuga C, Hudaidh A, Yasskiy A. Vascular endothelial dysfunction and mortality risk in patients with chronic heart failure. *Circulation*. 2005;111:310–314.
  42. Lee HY, Oh BH. Aging and arterial stiffness. *Circ J*. 2010;74:2257–2262.
  43. Chow B, Rabkin SW. The relationship between arterial stiffness and heart failure with preserved ejection fraction: a systemic meta-analysis. *Heart Fail Rev*. 2015;20:291–303.
  44. Zieman SJ, Melenovsky V, Kass DA. Mechanisms, pathophysiology, and therapy of arterial stiffness. *Arterioscler Thromb Vasc Biol*. 2005;25:932–943.
  45. Yasmin, Wallace S, McEniery CM, Dakham Z, Pusalkar P, Maki-Petaja K, Ashby MJ, Cockcroft JR, Wilkinson IB. Matrix metalloproteinase-9 (MMP-9), MMP-2, and serum elastase activity are associated with systolic hypertension and arterial stiffness. *Arterioscler Thromb Vasc Biol*. 2005;25:372–378.
  46. Wilkinson IB, Franklin SS, Cockcroft JR. Nitric oxide and the regulation of large artery stiffness: from physiology to pharmacology. *Hypertension*. 2004;44:112–116.
  47. McEniery CM, Wallace S, Mackenzie IS, McDonnell B, Yasmin Newby DE, Cockcroft JR, Wilkinson IB. Endothelial function is associated with pulse pressure, pulse wave velocity, and augmentation index in healthy humans. *Hypertension*. 2006;48:602–608.
  48. Brandes RP, Fleming I, Busse R. Endothelial aging. *Cardiovasc Res*. 2005;66:286–294.
  49. Abeyrathna P, Su Y. The critical role of Akt in cardiovascular function. *Vascul Pharmacol*. 2015;74:38–48.
  50. Michaud SE, Dussault S, Groleau J, Haddad P, Rivard A. Cigarette smoke exposure impairs VEGF-induced endothelial cell migration: role of NO and reactive oxygen species. *J Mol Cell Cardiol*. 2006;41:275–284.
  51. Masaki N, Sato A, Horii S, Kimura T, Toya T, Yasuda R, Namba T, Yada H, Kawamura A, Adachi T. Usefulness of the d-ROMs test for prediction of cardiovascular events. *Int J Cardiol*. 2016;222:226–232.
  52. Kobayashi T, Nemoto S, Ishida K, Taguchi K, Matsumoto T, Kamata K. Involvement of CaM kinase II in the impairment of endothelial function and eNOS activity in aortas of Type 2 diabetic rats. *Clin Sci*. 2012;123:375–386.
  53. Murthy S, Koval OM, Ramiro Diaz JM, Kumar S, Nuno D, Scott JA, Allamargot C, Zhu LJ, Broadhurst K, Santhana V, Kutschke WJ, Irani K, Lamping KG, Grumbach IM. Endothelial CaMKII as a regulator of eNOS activity and NO-mediated vasoreactivity. *PLoS One*. 2017;12:e0186311.
  54. Adapala RK, Talasila PK, Bratz IN, Zhang DX, Suzuki M, Meszaros JG, Thodeti CK. PKC $\alpha$  mediates acetylcholine induced activation of TRPV4-dependent calcium influx in endothelial cells. *Am J Physiol Heart Circ Physiol*. 2011;301:H757–H765.
  55. Kitayama J, Kitazono T, Ibayashi S, Wakisaka M, Watanabe Y, Kamouchi M, Nagao T, Fujishima M. Role of phosphatidylinositol 3-kinase in acetylcholine-induced dilatation of rat basilar artery. *Stroke*. 2000;31:2487–2493.
  56. Zecchin HG, Priviero FB, Souza CT, Zecchin KG, Prada PO, Carvalho JB, Velloso LA, Antunes E, Saad MJ. Defective insulin and acetylcholine induction of endothelial cell-nitric oxide synthase through insulin receptor substrate/Akt signaling pathway in aorta of obese rats. *Diabetes*. 2007;56:1014–1024.
  57. Dudzinski DM, Michel T. Life history of eNOS: partners and pathways. *Cardiovasc Res*. 2007;75:247–260.
  58. Balligand JL, Feron O, Dessy C. eNOS activation by physical forces: from short-term regulation of contraction to chronic remodeling of cardiovascular tissues. *Physiol Rev*. 2009;89:481–534.

# **SUPPLEMENTAL MATERIAL**

## **Data S1.**

### **Supplemental Introduction**

The experimental method was referring to our previous studies,<sup>1,2</sup> in which freshly isolated endothelial cells were obtained by wire-abrasion of upper-arm vein. However, this is the first study to use endothelial cells collected from radial catheter sheath. The non-invasive assessment enables us to measure and compare endothelial insulin resistance in many patients. Therefore, 1) validation of anti-phospho-eNOS antibody, and 2) optimization of quantifying immunofluorescence intensity should be reconfirmed. Furthermore, positive control and negative control were encouraged for validating the quantification of immunofluorescence intensity. For the reasons, we added the following data, which support the effectiveness of our method and the results.

In addition, we attached the solution path of the adaptive Lasso model to show the process of selecting the independent factors for the cardio-ankle vascular index (CAVI).

## **Supplemental Methods**

### **Endothelial cells**

Human umbilical vein endothelial cells (HUVECs) of passage 3-4 were cultured in dish or 4-well chamber slides. The cells were starved for 24 hours with serum-free medium. The cells were collected with lysate buffer for western blotting or fixed with 4% paraformaldehyde for immunofluorescence microscopy.

### **Western blot analysis**

Proteins were subjected to 4 to 12% gradient gels (Invitrogen) and transferred to polyvinylidene difluoride membranes. Membranes were initially blocked (Blocking one, Nacalai Tesque, Kyoto, Japan) for 1 hour. Membranes were cut and probed in blocking buffer containing primary antibodies of 1:2000 dilution: phosphorylated eNOS at serine 1177 (GeneTex, Irvine, CA), followed by the appropriate horseradish peroxidase–conjugated secondary antibody.

Immunoreactions were visualized with SuperSignal® West Dura Extended Duration Substrate (Thermo Scientific). Membranes were stripped (WB Stripping Solution, Nacalai Tesque) for 30 minutes at room temperature were

probed with phosphorylated eNOS at serine 1177 (1:1000 dilution; Cell Signaling, Danvers, MA), eNOS/NOS Type III (1:2000 dilution; BD Biosciences, San Jose, CA). The other cuts of membranes were probed with phosphorylated Akt at serine 473, total Akt [1:1000 dilution; Cell Signaling (CST)], GAPDH antibodies of 1:1000 dilution to verify equal protein loading. The bands were quantified by densitometry.

### **Immunohistochemistry**

The method was described in our previous paper.<sup>3</sup> Briefly, formalin-fixed saphenous veins were embedded in paraffin, and washed with xylene, 100% ethanol, 95% ethanol, and water for slide deparaffinization. Endogenous peroxidase was removed by treatment with 3% H<sub>2</sub>O<sub>2</sub> for 5 minutes and washing it under running water for 5 minutes. Antigen retrieval was performed by using the autoclave method (20 minutes at 121°C) and a citrate buffer (10 mmol/L, pH 8). After cooling, the plate was washed with phosphate-buffered saline (1.37 mol/L NaCl, 27 mmol/L KCl, 81 mmol/L Na<sub>2</sub>HPO<sub>4</sub>, 12 H<sub>2</sub>O, 14.7 mmol/L KH<sub>2</sub>PO<sub>4</sub>) and blocking was performed for 60 minutes using Blocking One (1/5, Nacalai Tesque). Incubation was performed overnight at 4°C with the primary



antibody (p-eNOS Ser1177, 1:50, GTX50212, GeneTex). After washing with phosphate-buffered saline, the secondary antibody (Histofine R Simple Stain MAX PO MULTI, Nichirei Bioscience Inc.) was reacted for 1 h. Finally, 3,3'-diaminobenzidine was added and allowed to react for 10 minutes, before the samples were dehydrated, penetrated, and re-sealed.

### **Assessment of protein expression by quantitative Immunofluorescence**

Fixed sample slides were thawed and rehydrated with PBS containing 50 mmol/L glycine (Sigma) for 10 minutes. The cells on the slides were permeabilized with 0.1% Triton X-100, and nonspecific binding sites were blocked with 0.5% BSA. The slides were incubated overnight at 4°C with primary antibodies against the following targets: p-eNOS Ser1177 (1:200 dilution; GeneTex). All of the slides were double-stained with an anti-von Willebrand Factor (vWF) antibody (1:300 dilution; Invitrogen, Carlsbad, CA), or eNOS/NOS Type III (1:200 dilution; BD Biosciences) for identification of endothelial cell. After the incubation, the slides were washed and incubated for 1 hour at 37°C with corresponding Alexa Fluor-488 and Alexa Fluor-594 antibodies (1:200 dilution; Invitrogen). The slides were washed again and

mounted under glass coverslips with Vectashield containing DAPI for nuclear identification (Vector Laboratories, Burlingame, CA).

Slide images of a fluorescence microscope at × 20 magnification were captured (KEYENCE, Osaka, Japan). Exposure time was constant, and image intensity was corrected for background fluorescence. Fluorescent intensity was quantified by a software (KEYENCE, Osaka, Japan). For each protein of interest, fluorescent intensity was quantified in 20 cells from each slide and averaged.

### **Making lentivirus vector expressing short-hairpin RNA to knock-down eNOS.**

The target sequence (GGAACAGCACAAGAGTTA) was designed from Human NOS3 mRNA sequence (NM\_000603.4). This sequence recognizes all isoforms of NOS3 and substantially (5 nt) differs from potential off-target sequences by Blast analysis. ShRNA expressing lentivirus was made as published by us before.<sup>4</sup>

## **Supplemental Results**

### **Validation of anti-phospho-eNOS antibody used in the study**

The method of this study is highly dependent on the quality of antibody. The western blot with anti-p-eNOS Ser1177 antibody (GTX50212, GeneTex), which were used for immunofluorescence in the study, exhibits a single band just below 150 kD (Figure S1A). The same membrane was stained with anti-p-eNOS Ser1177 antibody (CST #9571) (Figure S1B) and subsequently with anti-total-eNOS antibody (BD 610297) (Figure S1C). The bands located same molecular weight. Therefore, we confirmed that changes of immunofluorescent intensity come from the protein of this band. Thus, the anti-p-eNOS antibody (GTX50212) is available for quantification of immunofluorescent intensity.

Figure S2 shows the sections of a human saphenous vein harvested from a same patient during coronary artery bypass grafting. The intima was stained by anti-p-eNOS antibody (GTX50212) (left) as same as anti-total-eNOS antibody (BD 610297) (right). The image of vascular endothelial growth factor (VEGF)-stimulated section is also available in our recent paper.<sup>3</sup> The intensity was thickened by 30 minutes stimulation of VEGF.

### **Optimization of quantifying immunofluorescence intensity**

HUVECs were cultured in 4-well chamber slides (Figure S3A). The cells were starved for 24 hours with serum-free medium and fixed with 4% paraformaldehyde at each time point after stimulation. From the results, the timing of evaluating immunofluorescence intensity was considered appropriate at 30 minutes for insulin, VEGF, and 15 minutes for ACh (Figure S3B).

Figure S4A shows the immunoblotting of the HUVECs with p-eNOS Ser1177 (GTX50212). eNOS was activated after increase of p-Akt Ser473 (CST #4060). The comparison between western blotting and immunofluorescence is shown in Figure S4B. The inter-class correlation was 0.928 ( $p = 0.004$ ). The result indicates that the quantification of immunofluorescent intensity is functional to detect the change of p-eNOS Ser1177.

### **Validation of method with eNOS knockdown HUVECs**

We created HUVECs with eNOS knock-down (KD) for negative controls to test our assessment of immunofluorescent microscopy. The images of HUVECs after insulin stimulation treated by KD were shown in Figure S5A. The total

eNOS (red) was reduced by KD. The p-eNOS Ser1177 (GTX50212, green) was extinguished regardless of insulin stimulation.

Figure S5B shows the western blotting of HUVECs with or without KD. The bands of p-eNOS Ser1177 (GTX50212) was eliminated by KD. Thus, these results reconfirmed the validation of the antibody.

### **Positive control with serum-stimulation**

It was previously known that thrombin increases eNOS activation.<sup>5-7</sup> Figure S6A shows the increased immunofluorescent intensity of p-eNOS Ser1177 by culturing with human fresh serum for 30 minutes before fixation. The effect was not seen in the HUVECs treated by KD. The western blotting confirmed that p-eNOS Ser1177 increased by serum after augmentation of p-Akt Ser473 (Figure S6B)

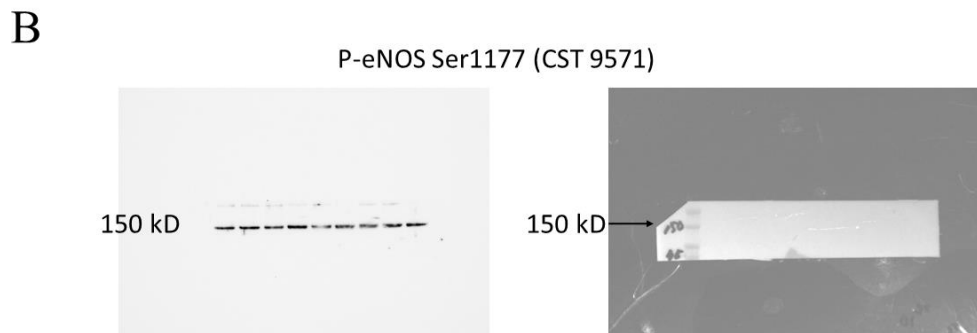
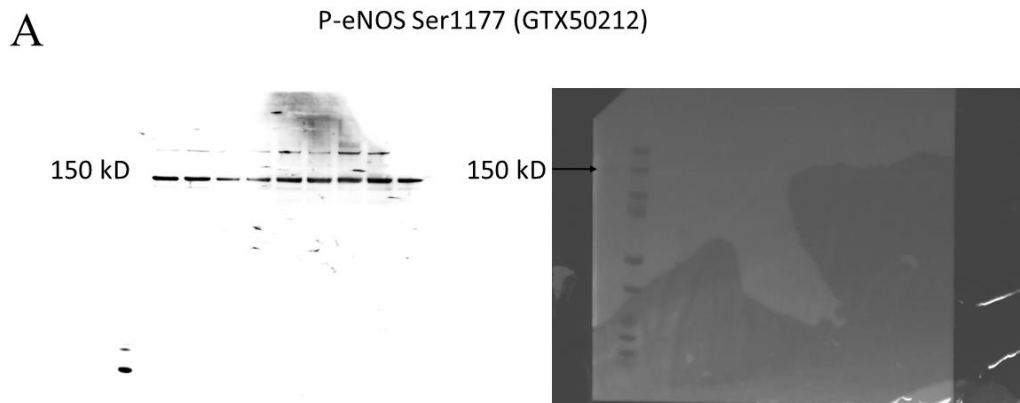
. This serum-stimulated increase of p-eNOS Ser1177 was absent by KD (Figure S6C) as same as other stimulations (Figure S6D). Therefore, we applied serum-stimulation to freshly isolated arterial endothelial cells as a positive control. The results were described in the main text (Figure 3).

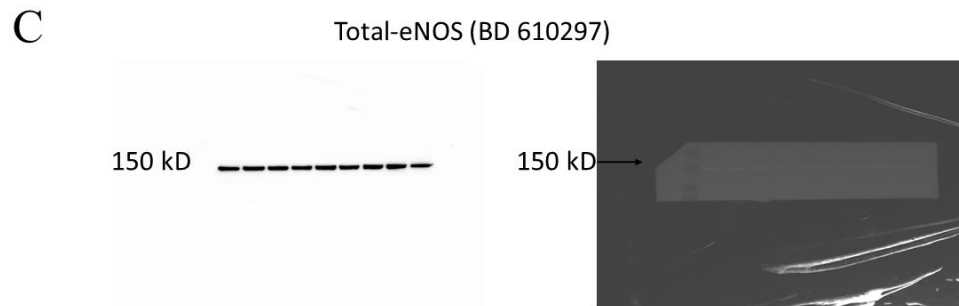


**The supplemental data of the adaptive Lasso regression for CAVI.**

Figure S7 shows the solution path of the adaptive Lasso regression model (model 3 in Table 4) described by JMP pro. version 13.1.0 (SAS Institute Japan, Tokyo).

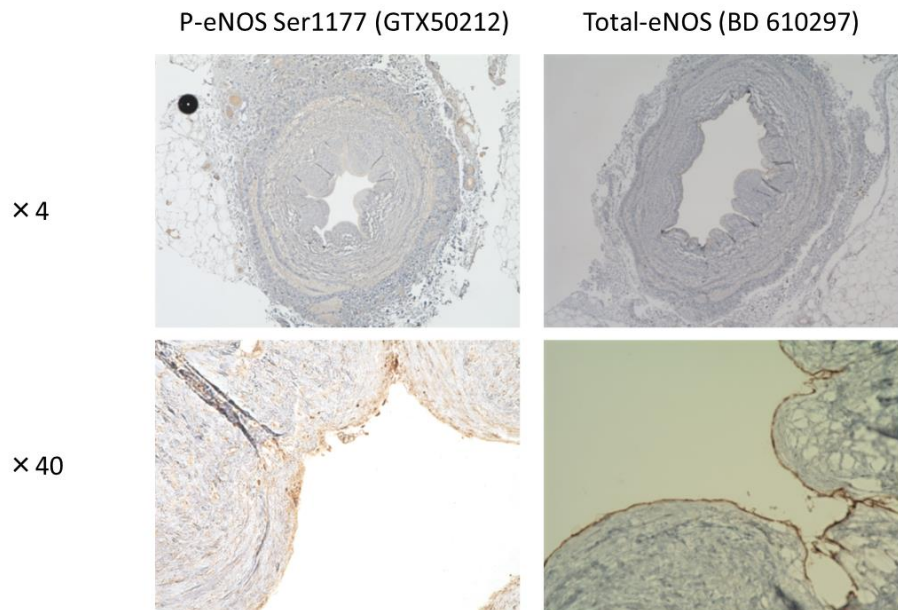
**Figure S1. The validation of anti-p-eNOS antibody by western blotting.**





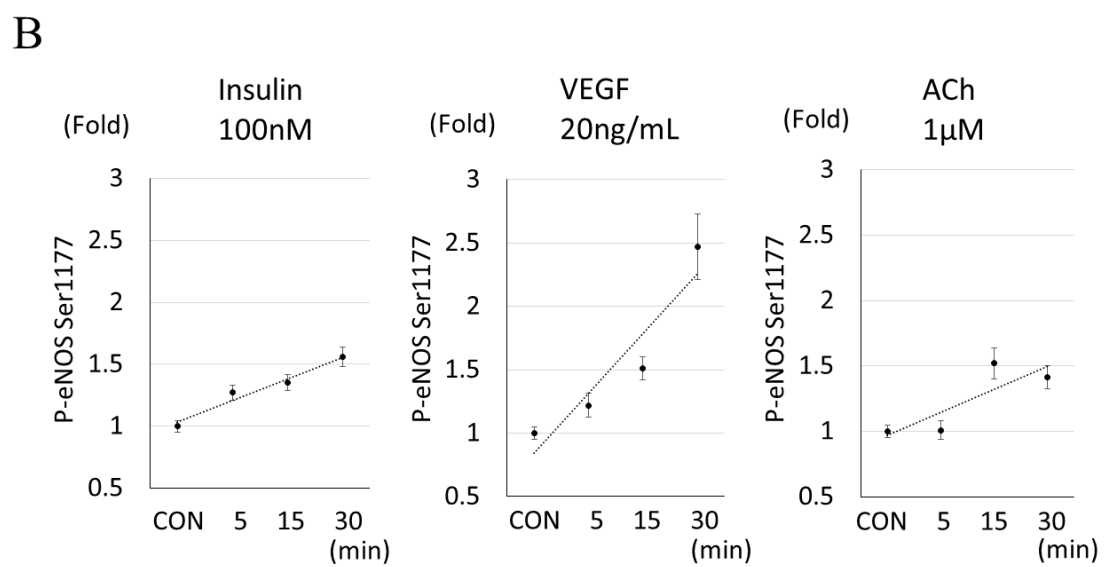
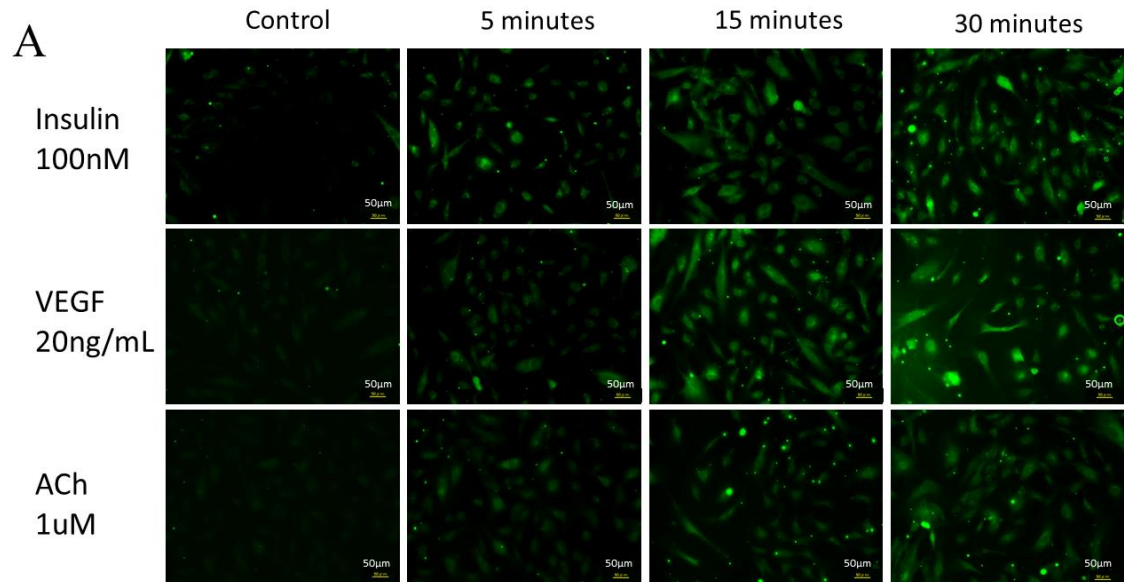
A: The western blot with anti-p-eNOS Ser1177 antibody (GTX50212), B: anti-p-eNOS Ser1177 antibody (CST #9571), C: anti-total-eNOS antibody (BD 610297). The figures are a chemifluorescent image (left) and a digitizing image (right).

**Figure S2. The validation of anti-p-eNOS antibody by immunohistochemistry.**



The images show the location probed by the anti-p-eNOS Ser1177 antibody (GTX50212) (left) and anti-total-eNOS antibody (BD 610297) (right).

**Figure S3. Optimal timing for evaluating immunofluorescent intensity.**

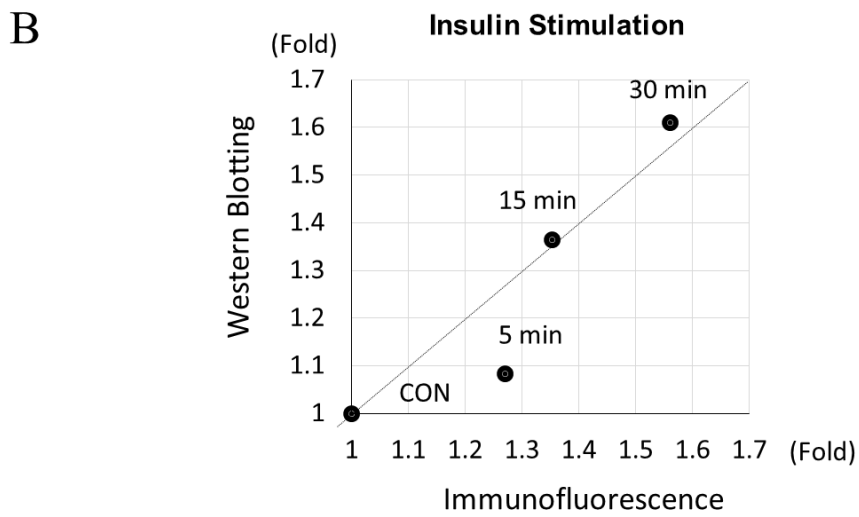
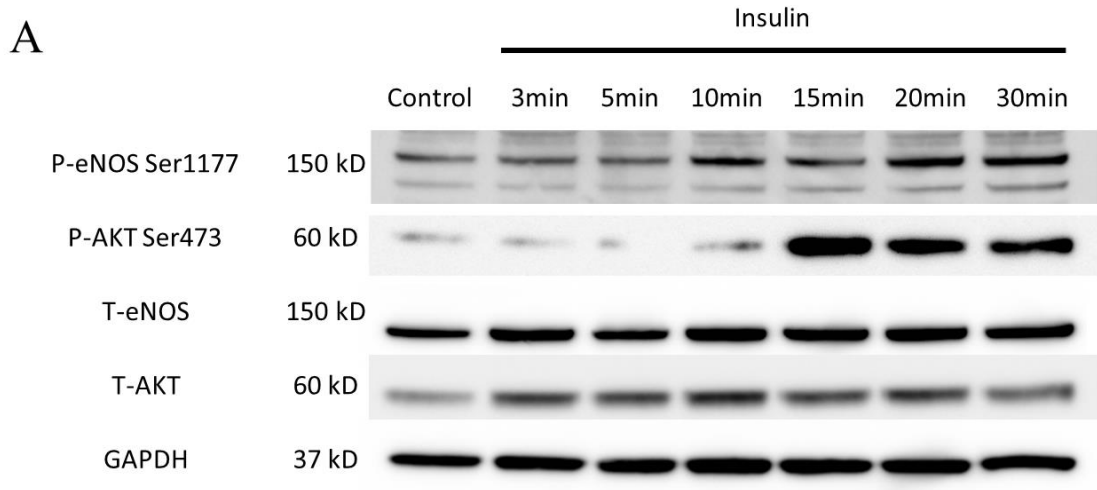


A: The immunofluorescent images with anti-p-eNOS antibody (1:200, GTX50212). Control slides had no stimulation. The times after each stimulation were indicated above the pictures.

B: The graphs of the intensities (ratio to average of control, mean  $\pm$  standard error).

VEGF, vascular endothelial growth factor; ACh, acetylcholine.

**Figure S4. The relationship between intensities of western blotting and immunofluorescence of HUVECs after insulin-stimulation.**

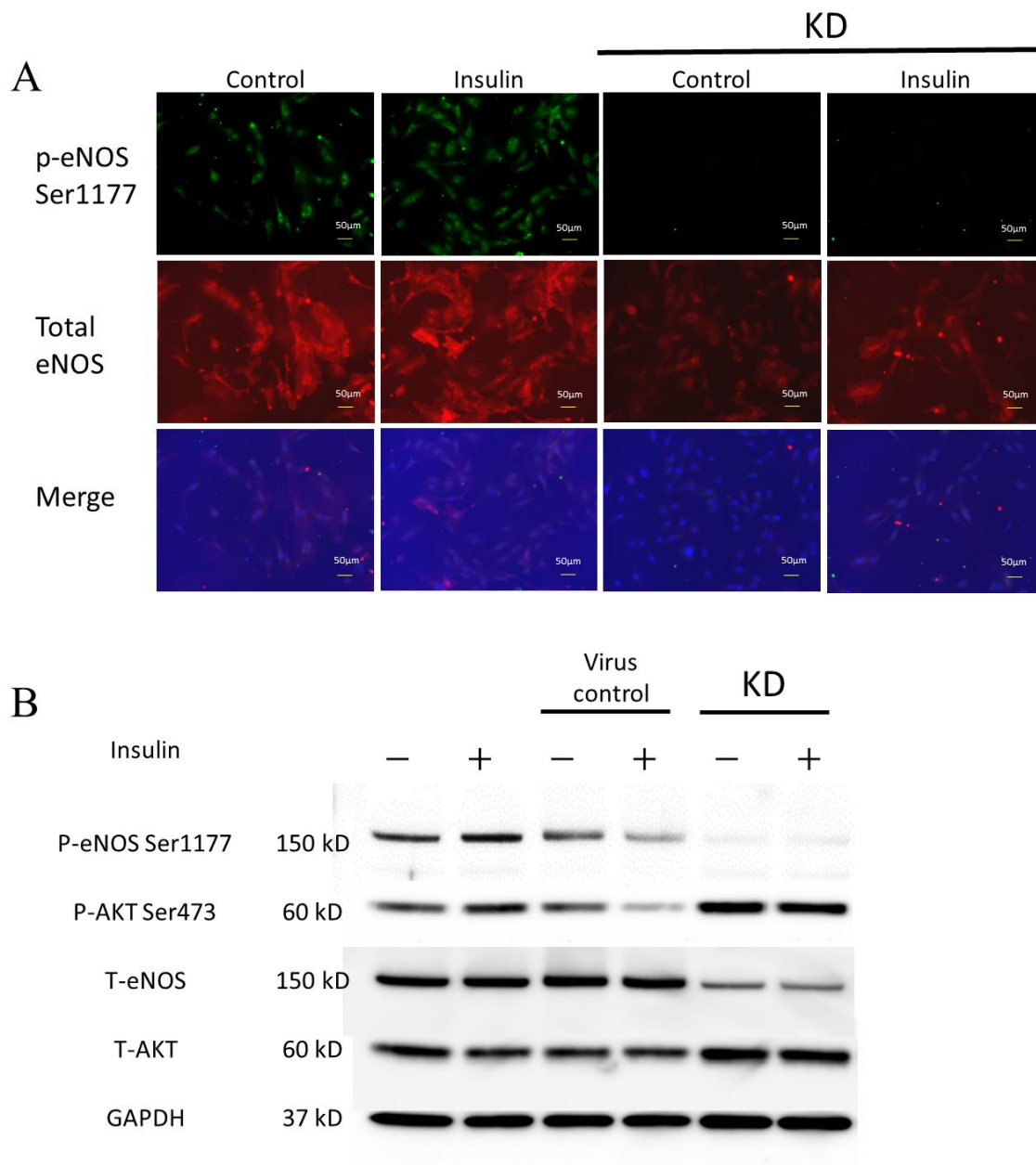


The immunoblotting image (A) shows gradual increase of p-eNOS Ser1177 after rise of p-Akt Ser473 by addition of insulin 100 nM. The plots (B) shows the

positive correlation of the results from western blotting and immunofluorescence.



**Figure S5. Elimination of p-eNOS Ser1177 by eNOS knockdown.**

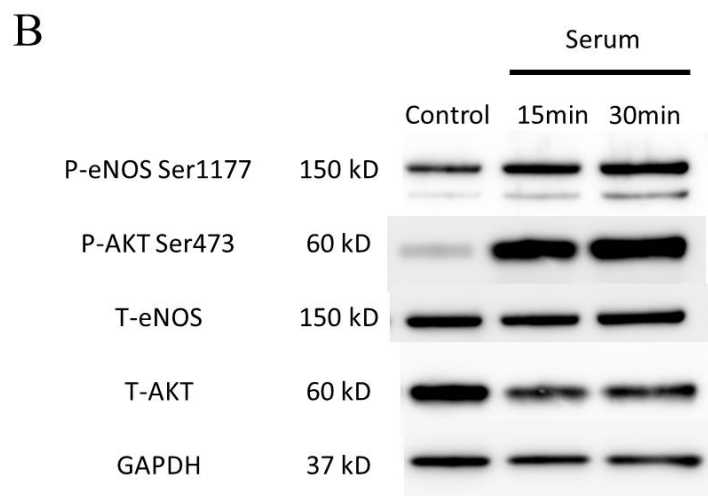
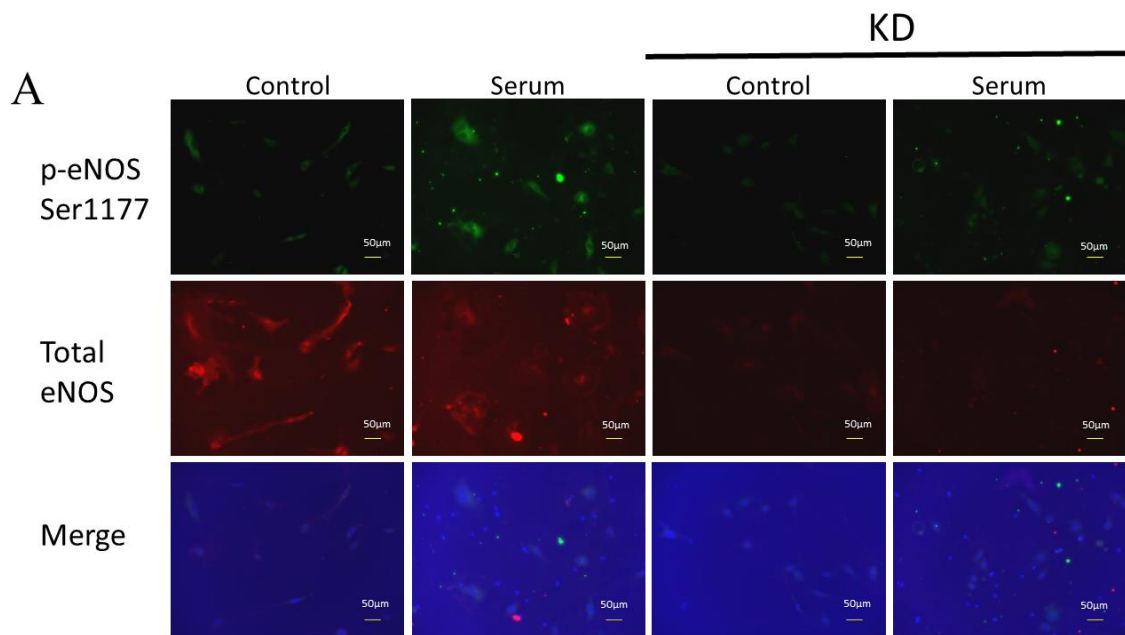


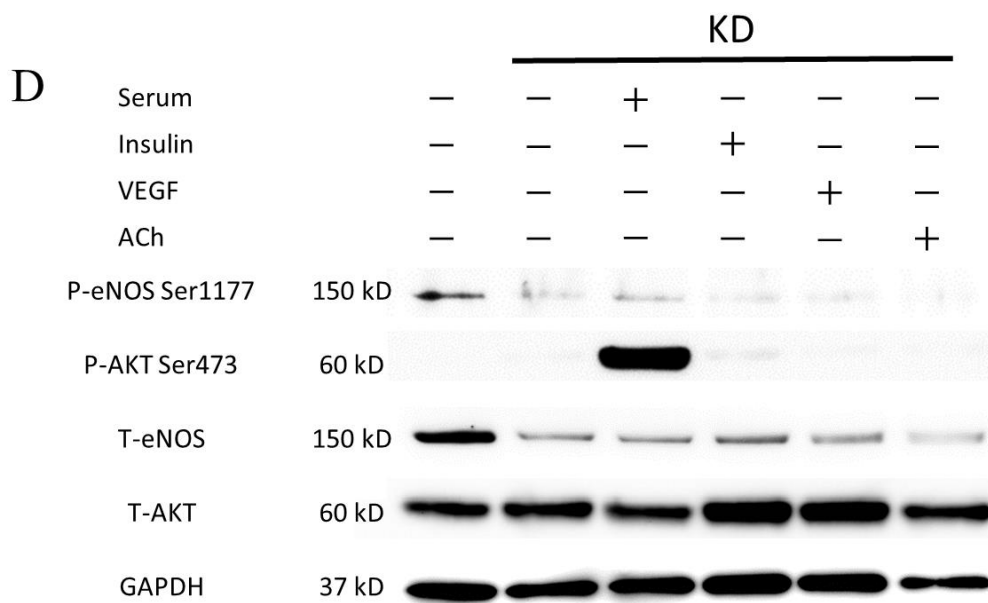
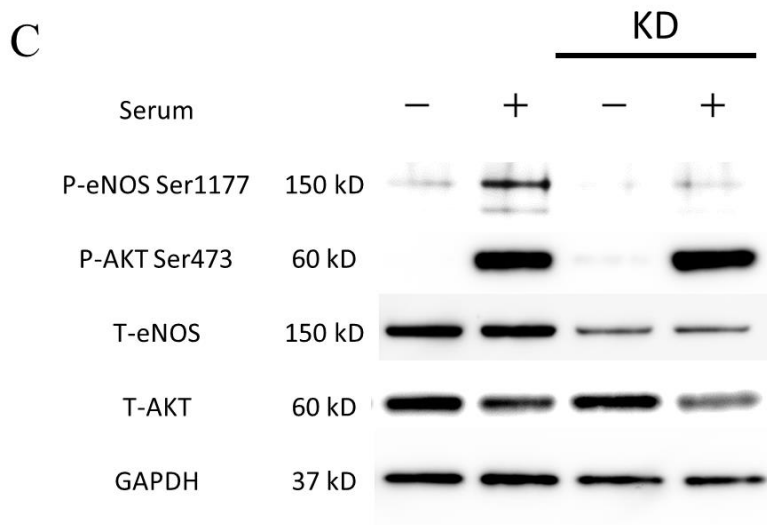
A: The immunofluorescent images with anti-p-eNOS antibody (GTX50212). B:

The western blotting. Control slides had no stimulation. Insulin stimulation was

100 nM 30 minutes. KD, eNOS knockdown.

**Figure S6. Augmentation of p-eNOS Ser1177 by serum-stimulation.**





A: The immunofluorescent images with anti-p-eNOS antibody (GTX50212). B:

The western blotting of time-course p-eNOS Ser1177 after serum-stimulation.

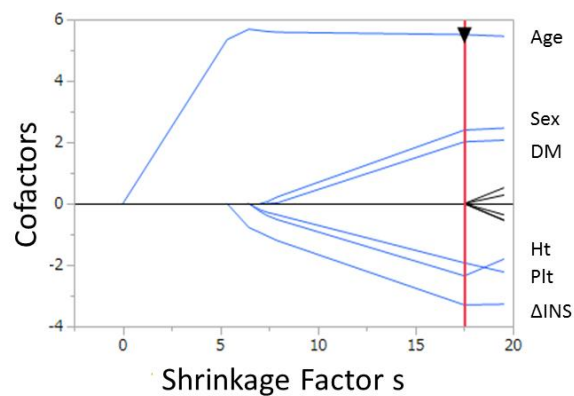
C: The western blotting showing the effects of KD on HUVECs with serum-

stimulation. D: The western blotting showing the effects of KD on HUVECs with other stimulations.

Control slides had no stimulation. Serum-stimulation was incubating with human fresh serum for 30 minutes. Insulin-stimulation was addition of insulin 100 nM for 30 minutes. VEGF-stimulation was 20 ng/mL for 30 minutes. ACh-stimulation was 1  $\mu$ M for 15 minutes.

KD, eNOS knockdown; VEGF, vascular endothelial growth factor; ACh, acetylcholine.

**Figure S7. Solution path.**



The original prediction formula was as follows;  $7.347962 + (-0.015367) \cdot \Delta\text{INS} + 0.0831406 \cdot \text{Age} + 0.869302 \cdot \text{Sex} + 0.6601768 \cdot \text{DM} + (-0.086475) \cdot \text{Ht} + (-0.043499) \cdot \text{Plt}$ .

The categorical variables are Sex (man 1, woman 0) and DM (yes 1, no 0).  $\Delta\text{INS}$ , percent change in insulin-induced p-eNOS at Ser1177; DM, diabetes mellitus; Ht, hematocrit; Plt, platelets.

## Supplemental References:

1. Tabit CE, Shenouda SM, Holbrook M, Fetterman JL, Kiani S, Frame AA, Kluge MA, Held A, Dohadwala MM, Gokce N, Farb MG, Rosenzweig J, Ruderman N, Vita JA, Hamburg NM. Protein kinase C- $\beta$  contributes to impaired endothelial insulin signaling in humans with diabetes mellitus. *Circulation*. 2013;127:86-95.
2. Bretón-Romero R, Feng B, Holbrook M, Farb MG, Fetterman JL, Linder EA, Berk BD, Masaki N, Weisbrod RM, Inagaki E, Gokce N, Fuster JJ, Walsh K, Hamburg NM. Endothelial Dysfunction in Human Diabetes Is Mediated by Wnt5a-JNK Signaling. *Arterioscler Thromb Vasc Biol*. 2016;36:561-569.
3. Yamada T, Adachi T, Ido Y, Masaki N, Toya T, Uchimuro T, Nishigawa K, Suda H, Osako M, Yamazaki M, Takanashi S, Shimizu H. Preserved Vasoconstriction and Relaxation of Saphenous Vein Grafts Obtained by a No-Touch Technique for Coronary Artery Bypass Grafting. *Circ J*. 2018;83:232-238.
4. Lan F, Cacicedo JM, Ruderman N, Ido Y. SIRT1 modulation of the acetylation status, cytosolic localization, and activity of LKB1. Possible role in AMP-activated protein kinase activation. *J Biol Chem*. 2008;283:27628-35.
5. Thors B, Halldórsson H, Jónsdóttir G, Thorgeirsson G. Mechanism of thrombin mediated eNOS phosphorylation in endothelial cells is dependent on ATP levels after stimulation. *Biochim Biophys Acta*. 2008;1783:1893-902.
6. Motley ED, Eguchi K, Patterson MM, Palmer PD, Suzuki H, Eguchi S. Mechanism of endothelial nitric oxide synthase phosphorylation and activation by thrombin. *Hypertension*. 2007;49:577-83.
7. Touyz RM. Regulation of endothelial nitric oxide synthase by thrombin. *Hypertension*. 2007;49:429-31.